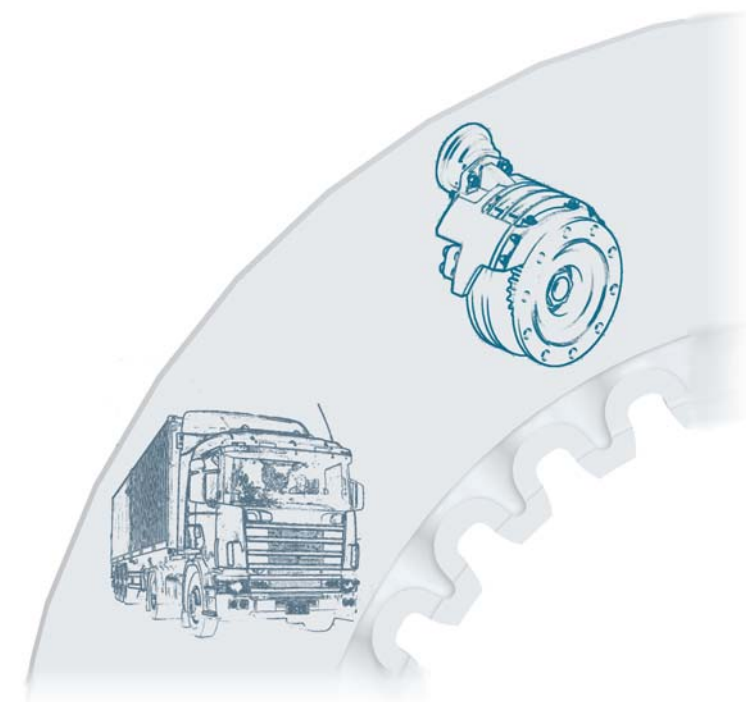




CRACK PROPAGATION IN FIXED CALLIPER BRAKE DISCS



Martin Norlander

Crack propagation in fixed calliper brake discs

Division of Solid Mechanics

Martin Norlander

Master's Dissertation

Department of Mechanical Engineering
Solid Mechanics

ISRN LUTFD2/TFHF-05/5110-SE(1-66)

CRACK PROPAGATION IN FIXED CALLIPER BRAKE DISCS

Master's Dissertation by

Martin Norlander

Supervisors

Göran Stensson, Haldex, Sweden

Joakim Gripemark, Haldex, Sweden

Håkan Hallberg, Div. of Solid Mechanics, Lund University, Sweden

Copyright © 2005 by Div. of Solid Mechanics,

Haldex, Martin Norlander

Printed by KF Sigma, Lund, Sweden

For information, adress:

Division of Solid Mechanics, Lund University, Box 118, SE-221 00 Lund, Sweden

Homepage: <http://www.solid.lth.se>

Abstract

This masters thesis describes work made in order to make sure that the brake discs used in *Fixed Calliper Brakes*, under development by *Haldez Brake Products*, are failsafe with respect to crack growth.

The previous development of the brakes has resulted in a disc geometry that shows limited plastic deformation in calculations, and good resistance to cracking in tests. This thesis aims to increase the knowledge considering crack growth, the methods used to analyse it in order to make predictions, and techniques which can be used to prevent it.

Finite element, FE, calculations are made using a non linear material model for grey cast iron and submodelling of the crack vicinity. A service life prediction is made using Paris' law together with results from the FE-calculations.

The calculations show that the disc with an initial defect of size and shape that is possible to occur can have a service life of 500 000 km.

Acknowledgements

This report is a result of a master thesis work made during the autumn of 2004. The project was initiated by Haldex Brake Products in Landskrona and it is carried out in close cooperation with the company. The thesis work is made at the Division of Solid Mechanics at Lund Institute of Technology, Lund University.

I would like to express my gratitude to my supervisors at Haldex: Göran Stensson and Joakim Gripemark. I would like to thank my examiner at the Division of Solid Mechanics, Niels Saabye Ottosen for guiding me into the interesting world of solid mechanics. Furthermore I would like to thank my supervisor at Solid Mechanics, Håkan Hallberg for his advice and support. I would also like to thank Ludwig Ljungberg for correcting the language of this report and Mattias Wallin for calculation results used during the work.

Martin Norlander

Contents

1	Introduction	1
1.1	Background	1
1.2	The project description	2
1.3	Earlier work done at Haldex	3
1.4	Overview	4
2	Crack intensity factors	6
2.1	K -factor	6
	FEM	9
2.2	J contour integral	10
	FEM	12
2.3	Choice of method	12
3	Material model for cast iron	14
3.1	Grey cast iron	14
3.2	Fatigue behaviour	15
3.3	Overloading	17
3.4	ANSYS cast iron material model	18
3.5	Plastic shakedown	22
4	Modelling	24
4.1	First simplified model	24
	Loads	24
	Meshing	27
	Submodel	28
	Results	28
4.2	Second model	29

Loads	30
Meshing	31
Solution schedule	31
Export and import	33
Results	34
5 Discussion	37
6 Improvements	40
6.1 Design criterion	40
6.2 Improvements in design	42
6.3 Overloading	42
7 Summary and conclusions	44
7.1 Summary	44
7.2 Conclusions	44
7.3 Future Work	45
References	47
A Material model	49
B Testing	52
C ANSYS APDL files	55
All	56
Spline	56
Submodel_rad	57
Boundary	60
SplineII	61
BoundaryII	61

Outpt 63
Post 65

1 Introduction

1.1 Background

For many years drum brakes have been the only type used on heavy vehicles, the last decade however disc brakes are fitted to an increasing share of new trucks, trailers and buses. The main reason for using disc brakes is the demand for increased brake torque offering a decrease in braking distance. There is still a big difference between the times for stopping a heavy truck and a passenger car. This is one of the main reasons for Haldex to work on a new brake concept: *The Fixed Calliper Brake* with double discs. The calliper contains the brake cylinder and the brake pads; it is the part of the brake that is fixed to the vehicle and hinders the rotation of the wheels when braking. The Fixed Calliper Brake has two floating discs fitted to the hub via a spline, this makes it possible for the discs to move in axial direction instead of the sliding of the calliper on slide pins, see figure 1. The elimination of calliper movement makes it possible to decrease the total weight of the brake assembly. At the same time it is possible to increase the brake torque due to the two extra friction surfaces per wheel compared to a conventional disc brake.

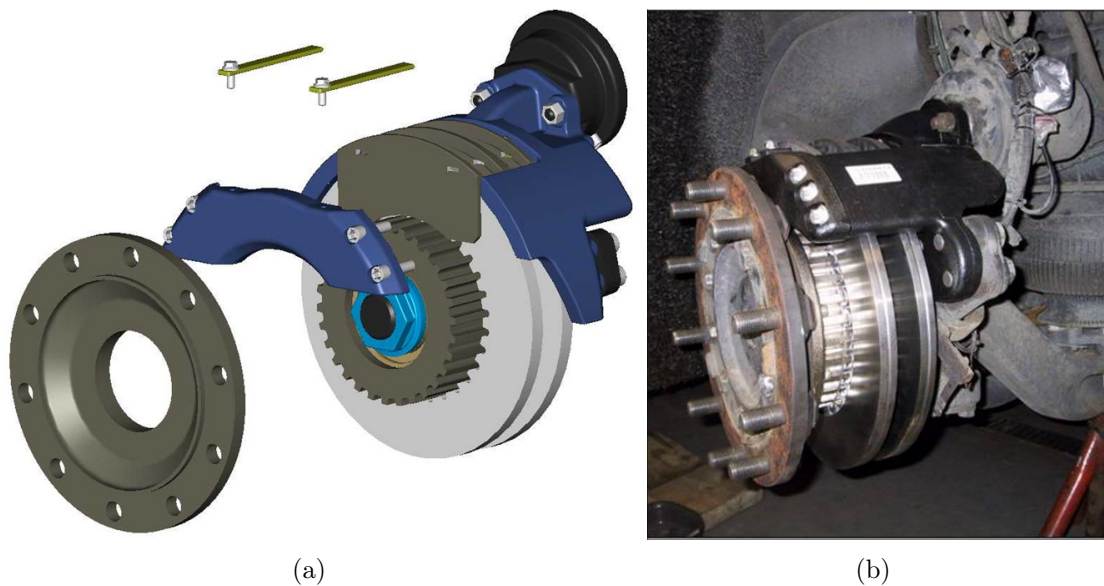


Figure 1: The Fixed Calliper Brake with double discs.

The slide pins have been a big source of problems occurring on conventional disc brakes, see figure 2. The main problem is callipers getting stuck on the pins due to corrosion or other reasons creating an increase in friction. This lack of calliper movement leads to increased wear of brake pads and discs, and thus to a rise in maintenance costs. The loss in function

arising from the corrosion is an even more severe problem which might be overcome by using the Fixed Calliper Brake.

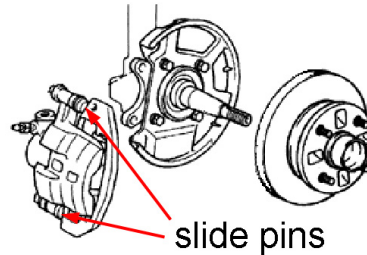


Figure 2: A conventional brake assembly.

Normally brake discs (and drums) are made of grey cast iron, a material with quite low strength. The use of grey cast iron is due to the good castability and the good thermal conduction.

1.2 The project description

The Fixed Calliper Brake has a failure mode that differs quite a lot from conventional disc brakes. While conventional discs, with the shape of a top hat, are destroyed by radial cracks originating mainly from the pulsating heat load when the discs move through the calliper and get a rapid heat rise passing the brake pads. The steep thermal gradients created are the origin for surface cracks in the discs. This problem is almost totally avoided with the Fixed Calliper Brake because this brake does not have the disc fixed to the cool and stiff hub, and the discs are therefore free to expand a lot more than the conventional ones. The problems with these discs are cracks originating in the spline at the inner radius of the disc; these cracks are potentially more dangerous than the surface cracks because the risk of a total failure is increased, and experiments carried out at Haldex has shown that these cracks grow faster than surface cracks.

The purpose of this thesis is to calculate how long it will take from the origin of a crack, from either a material defect or from errors made at assembling or handling the discs, to the total failure. When the mechanism of crack growth in the discs is understood, and the parameters affecting it, it is time to work on minimising the crack growth. The work minimising the crack growth must be concentrated to changes in the disc geometry since changing other parameters is expensive and the effort doing it can easily get too extensive to be covered by a master thesis. Some studies concerning the methods of manufacturing the discs will although be made.

The method to use calculating what stresses occur in the discs is mainly the *Finite Element Method*, FEM, this has been done to a great extent at Haldex in earlier works,

see chapter 1.3. The calculation program used at Haldex is ANSYS and this program is going to be used through out this thesis work as well. Most methods concerning crack growth assumes a linear material model, this however does not describe cast iron very well. Calculations and tests have showed that in order to get good results you have to use a better material model that is nonlinear, and considers the different behaviour of cast iron in compression and tension. The way to get around the problem with the two differing requirements on the material model is to assume that after some brake cycles there will be a *plastic shakedown* (see chapter 3.5) and there will be no further significant plasticity in the discs. This assumption has shown to be reasonable in the tests performed.

Modelling of the crack zone will be done with conventional methods in the area of fracture mechanics. These methods include sub modelling of the crack zone with mesh refinement, and the use of singularity elements at the crack tip. The work will be concentrated on linear fracture mechanics for simplicity and to get accuracy in the results as the elastic plastic area of fracture mechanics is not that developed. Another reason is the difficulty to find material parameters, this makes it hard to analyse results developed in nonlinear calculations.

1.3 Earlier work done at Haldex

The work made at Haldex has been concentrated to minimising crack initiation in the Fixed Calliper Brake discs. When tests of the first spline geometries showed fast initiation of cracks and a fast crack growth, efforts were made to minimize these problems. It turned out that the problems occurred due to strain concentrations in the cuts in the spline pattern.

The first calculations were made with a linear material model; these calculations showed bad agreement with experiments, as the calculations showed far too high stresses. The peak stress values in these calculations were much greater than the yield strength for the material. Later the ANSYS multilinear kinematical material model with von Mises' yield criterion was used, this choice of model was made mostly due to the lack of a model that better described the material [1].

In version 6.1 of ANSYS the cast iron plasticity model was released [2], this model was used in later works. Using this material model and a couple of different load cases, including the one described in chapter 4.1, the location of the *maximum principal plastic strain* were found in discs with varying spline geometry. Efforts were made to minimize the maximum plastic strain; this work resulted in great reduction and a reposition of it to a more favourable position. The main difference in geometry was made to create a more even distribution of the stiffness in the spline and this way minimising the great difference in strain between stiff parts and more weak parts. In geometries with differing stiffness, the weak parts had to carry a lot more of the strain creating problems with crack initiation

and crack growth eventually leading to collapse of the discs.

The geometry showing best results in calculations is the one called *Wave Spline* where the material volume has been minimized inside the cogs, see figure 3. This geometry has shown good results both in calculations and in real tests. Both new discs and discs at the wear limit have passed tough tests. The tests have been done on discs without any defects. Defects can have a fatal effect on the strength of the discs and that is the reason for this work.



Figure 3: The *Wave Spline* geometry.

1.4 Overview

The chapters in the thesis include the following information:

Chapter 2 Theory used later used in the work. The theory is mainly about the stress intensity factors J and K and how they are implemented in FE-methodology. Some remarks about how to make life time predictions are also included.

Chapter 3 The material behaviour for grey cast iron especially with respect to the fatigue properties. The constitutive model used to describe the material in ANSYS is included in the chapter as well.

Chapter 4 Description of how the modelling work is made in FEM, the load and constraints used to represent the braking. The chapter also describes how the submodelling is carried out, and the special steps used to combine the nonlinear material behaviour with the linear crack intensity factor used.

Chapter 5 A discussion about what factors which possibly affected the results and their agreement with the reality.

Chapter 6 Description of what methods and requirements that shall be chosen when working with future improvements of the design, with respect to the crack formation

and growth. The chapter also includes proposed improvements in design and manufacture that might impede crack growth, and what is to be done in the future in order to improve the brake discs from a fracture mechanical point of view.

Chapter 7 A summary of the results achieved in the work and what conclusions that can be drawn from them. The chapter also includes proposals for further work in order to improve the brake discs.

Appendix A The material parameters used in the material model.

Appendix B Proposal on a lab-testing procedure which can be used in order to verify the results of the thesis, this chapter also includes results from the modelling made in order to create a comparison between calculations and real tests.

Appendix C A listing of the files used when making the calculations on the model with the real geometry of the disc.

2 Crack intensity factors

2.1 K -factor

There are three possible ways a crack can be loaded, these so called modes are shown in figure 4.

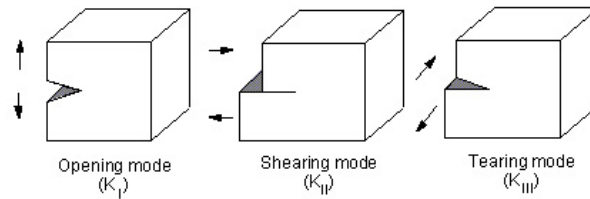


Figure 4: The three modes of loading that can be applied to a crack [3].

When studying the stresses in a body made in a material with linear behaviour with a crack loaded in one of the modes, you find that the stress approaches infinity moving towards the crack tip. The stress varies with $\frac{1}{\sqrt{r}}$ with r defined like in figure 5. The most common way to describe the stress concentration around a crack tip in a linear elastic material is through the stress intensity factor, K . Depending on which mode the crack is loaded in, the stress intensity factor is given an index I , II or III . This field of solid mechanics, considering crack growth, is called *linear elastic fracture mechanics*, *LEFM*.

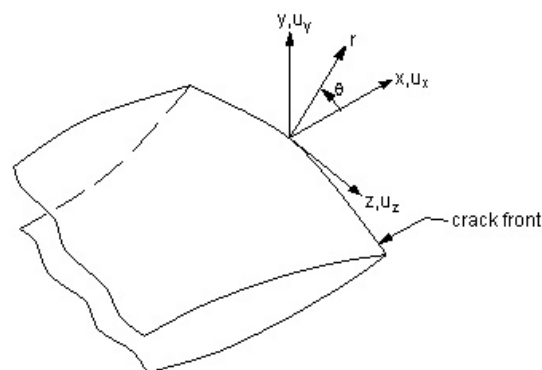


Figure 5: The coordinate system used in the calculations [3].

Assuming linear material behaviour the stress field near a crack tip loaded in mode I can

be described by:

$$\sigma_{xx} = \frac{K_I}{\sqrt{2\pi r}} \cos \frac{\theta}{2} \left[1 - \sin \frac{\theta}{2} \sin \frac{3\theta}{2} \right]$$

$$\sigma_{yy} = \frac{K_I}{\sqrt{2\pi r}} \cos \frac{\theta}{2} \left[1 + \sin \frac{\theta}{2} \sin \frac{3\theta}{2} \right]$$

$$\tau_{xy} = \frac{K_I}{\sqrt{2\pi r}} \cos \frac{\theta}{2} \sin \frac{\theta}{2} \cos \frac{3\theta}{2}$$

K_I is a parameter only dependent on the geometry of the cracked body and how it is loaded. These solutions are derived using, among others, the equilibrium equations and Airy's stress function in plane strain and plane stress. This was done by Westergaard the first time and the solutions are infinite sums where all the higher order terms have been neglected [4] (pages 54, 101-109). An even more general way to write the stress intensity for a body is:

$$K_I = f\sigma\sqrt{\pi a} \tag{1}$$

Where f is a function only depending on the geometry of the cracked body independent of the length of the crack a , and the stress perpendicular to the crack σ . This way to write the stress intensity, dividing it into a geometric part and a load part, makes it possible to gather f -values in tables for different geometries.

Normally tests are made to determine the fracture toughness, K_{Ic} , of the materials by using special test specimens of well defined size. The size of the specimens is important in order to guarantee that the material is loaded under plain strain conditions. When $K_I > K_{Ic}$ unstable crack propagation will occur in the loaded body [5]. The fracture toughness is highly dependent on the temperature, at elevated temperatures the material behaviour goes from brittle (which is assumed in linear fracture mechanics) to ductile. Cast iron has a brittle material behaviour at room temperature, and an increased ductility will only decrease the crack propagation, it is therefore conservative to assume the brittle behaviour even at elevated temperature.

When the stress intensity is cycled, the crack grows even when the loading is below K_{Ic} . This crack growth is described through Paris' law:

$$\frac{da}{dN} = C(\Delta K_I)^n$$

Where $\Delta K = K_{I,max} - K_{I,min}$ is the difference in stress intensity, C and n are material parameters. This equality makes it possible to calculate how much the crack grows in every load cycle $\frac{da}{dN}$. *Paris' law* is an idealisation of the linear part (B) of the crack growth curve in figure 6, the upper limit in this curve corresponds to K_{Ic} and the lower part corresponds to $K_{I,th}$. When the stress intensity factor is less than $K_{I,th}$ no crack growth will occur [6] (pages 295-296). It is important that the loading is in the linear part of the curve, and as a rule of thumb the requirements $K_{I,max} < 0.9K_{Ic}$ and $\Delta K_I > 1.1K_{I,th}$ can be used. The second of these expressions is used to make sure that crack closure phenomena not influence the results too much (see chapter 5) [7] (pages 251-252).

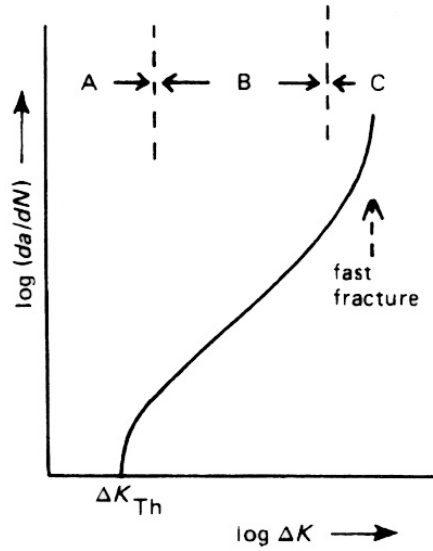


Figure 6: Typical crack growth under cyclic loading [6] (page 296).

Under the assumption that f is independent of crack length Paris' law can be integrated and the number of cycles necessary to make the crack grow from a_0 to a can be investigated [5, 8]:

$$N \approx \frac{a_0}{\left(\frac{da}{dN}\right)_0} \frac{1 - \left(\frac{a_0}{a}\right)^{n/2-1}}{n/2 - 1} \quad n \neq 2 \quad (2)$$

Index 0 indicates that the value is valid under initial crack conditions. If one more assumption is introduced, that the initial crack length, a_0 , is short related to the final crack length, a , makes the equality independent from a [8]:

$$N \approx \frac{a_0}{\left(\frac{da}{dN}\right)_0} \frac{1}{n/2 - 1} \quad n \neq 2, \quad a \gg a_0 \quad (3)$$

FEM

For some geometries and loadings there are closed form solutions to find in the literature, in most cases however closed form solutions are not possible to derive. This means that numerical methods have to be used.

For a crack loaded in mode I the displacement in the y -direction (perpendicular to the crack plane) is given by [4] (page 54):

$$u_y = \frac{K_I}{2\mu} \sqrt{\frac{r}{2\pi}} \sin \frac{\theta}{2} \left[\kappa + 1 - 2 \cos^2 \frac{\theta}{2} \right] \quad (4)$$

where

$$\begin{aligned} \kappa &= 3 - 4\nu && \text{plane strain} \\ \kappa &= \frac{3-\nu}{1+\nu} && \text{plane stress} \end{aligned} \quad (5)$$

and μ is the shear modulus:

$$\mu = \frac{E}{2(1 + \nu)}$$

This expression also follows from Westergaard's solution to the differential equation based on Airy's stress function. The higher order terms are neglected in this solution too; this means that it is only valid near the crack tip. Evaluating the equation for the displacement (4) at $\theta = \pm 180^\circ$ gives the displacement at the crack faces:

$$u_y = \frac{K_I}{2\mu} \sqrt{\frac{r}{2\pi}} (\kappa + 1)$$

Solving this expression for K_I in a full crack model gives:

$$K_I = \sqrt{2\pi} \frac{\mu}{1 + \kappa} \frac{|\Delta u_y|}{\sqrt{r}}$$

Where Δu_y is the motion of one crack face with respect to the other. The displacement of the nodes along the crack face is assumed to vary linear with r like:

$$\frac{|\Delta u_y|}{2\sqrt{r}} = A + Br$$

Let r approach 0

$$\lim_{r \rightarrow 0} \frac{|\Delta u_y|}{2\sqrt{r}} = A$$

Using the displacements of two nodes near the crack tip along the crack face to determine A the crack intensity factor in the first mode can be written as:

$$K_I = \sqrt{2\pi} \frac{2\mu A}{1 + \kappa}$$

The crack intensity factors in the other modes can be determined in the same way using the displacements u_x and u_z . Using this method the crack intensity factors are determined in ANSYS by the KCALC command [9].

2.2 J contour integral

Another way to describe the conditions near the crack tip is the J contour integral, named after Jim Rice. This integral can be used as a stress intensity parameter just like the stress intensity factor, K . The main advantage with the J integral is that it does not require linear material behaviour. When using the J integral methodology the material behaviour is approximated as non linear elastic. The value for J is determined in two dimensions through:

$$J = \int_{\Gamma} w dy - T_i \frac{\partial u_i}{\partial x} ds \quad (6)$$

Γ is a counter clock wise path at an arbitrary distance from the crack tip shown in figure 7. w is the strain energy density:

$$w = \int_0^{\epsilon_{ij}} \sigma_{ij} d\epsilon_{ij}$$

T_i is the components of the traction vector acting on the path, u_i is the displacement vector.

Just like the stress intensity factor, K , the J integral can be used to describe the stress-strain field near the crack tip. The origin for the integral was a way to describe the energy release rate when a crack grows under non linear material behaviour. In the special case when used under linear material properties, it can be shown that the J integral equals the

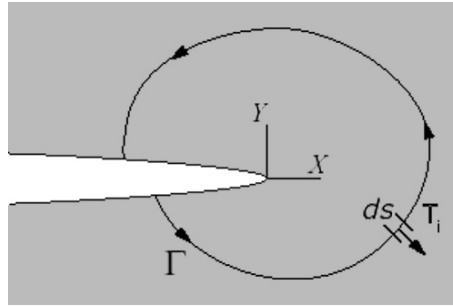


Figure 7: The coordinate system and the contour path when using the J integral methodology [10].

elastic energy release rate G . This parameter is normally used when studying linear elastic materials. This leads to a relationship between the two crack intensity factors K_I and J under linear premises:

$$J = \frac{K_I^2}{E}$$

J can also be used to define a material toughness, J_c , a value which defines when instable crack growth occurs.

The approximated behaviour of the material as non linear elastic creates constraints at the usage of the integral – repeated loadings are not described for most materials, but there is still a clear advantage over the fully linear K -factor. When used in three dimensions the crack tip is transformed to a crack front, this converts the path Γ into a tube surrounding the crack front. Defining the position along the crack front as a coordinate, η , and creating a local coordinate system with the origin in this point makes it possible to write a *weighted average* \bar{J} .

$$\bar{J}\Delta L = \int_{\Delta L} J(\eta)q d\eta$$

Where ΔL is the length of the studied crack front part, and $J(\eta)$ is the J integral value in the current point along the crack front. q is first introduced as an arbitrary function in two dimensions as a mathematical device that enables the transformation from a line integral to an area integral. The requirements on this function is merely that it must be smooth and defined at all points where the J integral is to be taken. It must also have the correct values at the boundaries (1 at the crack tip and 0 at the outer boundary in two dimensions). When the three dimensional formulation is created q can be taken as a function of the position along the crack front $q(\eta)$, this way q can be viewed like the *the*

virtual crack advance as a physical interpretation of the mathematical formulation. The three dimensional formulation can create a gain in accuracy. Later on however only the two dimensional formulation will be described in this thesis for simplicity [4] (pages 125-126, 578-583) .

FEM

The quantities in the equation (6) are easily obtained in all commercial FEM codes. The first one is the strain energy density, w , which can preferably be defined per element. This makes it possible to divide the strain energy for each element by the element volume, and in an easy manner derive the strain energy density. Creating a path around the crack tip, mapping the strain energy density to this path and integrate over the path length with respect to y , gives the first term in (6):

$$\int_{\Gamma} w dy$$

Defining a normal vector to the path Γ and using the stresses σ_x , σ_y and σ_{xy} makes it possible to get the traction vector working on the path.

The derivatives $\frac{\partial u_i}{\partial x}$ are defined by mapping the displacements to the path, then moving the path a distance in the x-direction in the local crack tip coordinate system. Knowing the distance dx the path is moved the makes it possible to approximate the derivatives. To refine the results the path can first be moved a distance $dx/2$ in the negative x -direction and then be moved an equal distance in the positive x -direction.

With the traction vector and the derivatives of the displacements known the second term in the equation (6) can be calculated [9].

$$- \int_{\Gamma} T_i \frac{\partial u_i}{\partial x} ds$$

2.3 Choice of method

Both stress intensity factors describe the stress field near the crack tip well, and both are easily used in post processing of FEM results. Even if the J integral is a good way to describe under which premises a crack propagates through a body, this method is not chosen in this thesis work. The choice for the K stress intensity factor is the fact that it is more established and therefore it is possible to find material parameters.

Cycled loading is not described in a satisfying manner by the J integral theory, even when it might describe it better than the linear K -factor under highly non linear premises. The

reason to choose the linear parameter, K , and its fatigue formulation, Paris' law, is the same in the case with cycled loadings: The possibility to find material parameters.

With the knowledge about the material behaviour after repeated loadings, described later in chapter 3.5, it is clear that the trade off is minor when choosing the K -factor when describing the crack growth.

3 Material model for cast iron

3.1 Grey cast iron

Cast iron is an iron with a surplus of carbon and with alloying elements to make it form desired structure when solidifying. The great share of carbon in cast iron (2.5-4%) is much more than the solution limit, this makes nucleation of carbon in form of graphite possible at slow cooling rates. To allow higher cooling rates and controlling the microstructure, alloying elements are added to the casting. Mainly silicon is added, this makes the stable formation of graphite flakes instead of cementite, Fe_3C , at higher cooling rates, and thus making an even distribution of the two phases occurring in the material. Phosphorus is also added to improve the fluidity of the iron, and to lengthen the solidification period.

The reason for using grey cast iron in brake discs is its superior resistance to heat checking, a fatigue phenomenon originating from pulsating heat loads which creates surface cracks in brake discs. The low cost of the material, the good castability, the relatively good thermal conduction and heat capacity, originating from the interconnected graphite flakes, are four more reasons for using grey cast iron. Furthermore grey cast iron has very good vibration damping which suppresses noise when braking; it also has excellent machinability since the chips break off easily at the graphite flakes [6, 11, 12] (pages 303-305; 385).

The graphite flakes work as stress raisers in the cast iron like tiny cracks, because of their low mechanical strength and brittleness. The graphite flakes causes local plastic flow when cast iron is loaded in tension, since the strength of the material is lower than under compression. The graphite flakes also gives the material a highly nonlinear behaviour when loaded in tension. This is due to the plastic deformation occurring near the flakes, stress concentrations give cast iron the plastic behaviour which can be seen in construction steels at much higher (global) stress levels. In compression however, the graphite flakes does not affect the mechanical behaviour that much and the strength and stress-strain behaviour of the material is mostly controlled by the matrix of ductile steel. The strength in compression is three to five times greater than the strength in tension [2]. The volume change described by the Poisson's ratio, ν , varies with stress and the behaviour differs in tension and compression. At low stresses the elastic value of the Poisson's ratio is 0.25, this value is decreasing with increasing stress in tension, and increasing with increasing stress in compression.

The small graphite flakes works like material defects and can be starting points for cracks; this gives grey cast iron poor fatigue properties. On the other hand the material is insensitive to notches mainly because of the distributed graphite flakes acting as defects. These even spread stress raisers makes the existence of a mark on the surface of less significance.

The cast iron used in brake discs at Haldex is in the lower strength classes due to high carbon content, the high carbon content enhances many of the desired properties, such as

%C	%Si	%Mn	%P	%S	%Cr	%Cu	%V	%Mo	%Sn	%La	%Zr
3.72	1.74	0.50	0.05	0.108	0.16	0.24	0.02	0.45	0.112	0.0085	0.03

Table 1: The GG15HC composition [13].

the thermal conductivity of the material, but lowers the strength. The material properties are often defined by the carbon equivalent, CE , defined as:

$$CE = \%C + \frac{1}{3}\%Si$$

The reason for this is the behaviour of the silicon as a graphite stabiliser in the cast iron. The GG15HC iron used in the brake discs has the composition defined in table 1. This composition gives a carbon equivalent of 4.3%.

It is hard to define the exact microstructure of the cast iron used, what is for sure is that the behaviour is mainly controlled by the graphite flakes. The amount of pearlite and ferrite is not reported by Fritz Winter GmbH [13], who is the material supplier of Haldex. This has no significance because the microstructure changes during use of the brakes, due to the elevated temperature during operation. The most probable is that the iron only contains ferrite, α , and graphite since an elevated temperature for a long time works as a heat treatment [11] (pages 381-385).

3.2 Fatigue behaviour

In an article written by J.H.Bulloch [14] the fatigue behaviour of grey cast iron is studied (defined as flake cast iron in the article). The material studied in the article differs little in composition from GG15HC. The carbon content is a little lower in the studied iron (3.28%) than in GG15HC. On the other hand the silicon content (2.14%) is higher in the studied iron and therefore the carbon equivalent is close to that of GG15HC (3.99%). The lower carbon content in the studied iron gives it a higher yield strength and toughness; this means that there can be a risk in applying the values from this article when making the calculations. Some caution is necessary when studying the results, but the difference in material composition is marginal and should not create any big issues. The testing was made by Bulloch on compact tension specimens, tests with such specimens gives K_I .

Bulloch shows in his article that in addition to the value ΔK_I the ratio between the minimum and maximum stress intensity R plays a major role in the crack growth rate.

$$R = \frac{K_{I,min}}{K_{I,max}} = \frac{\sigma_{min}}{\sigma_{max}}$$

The importance of the R -ratio is illustrated in figure 8. From this figure it can be seen that the R -ratio is of bigger importance than the amounts of pearlite/ferrite in the iron.

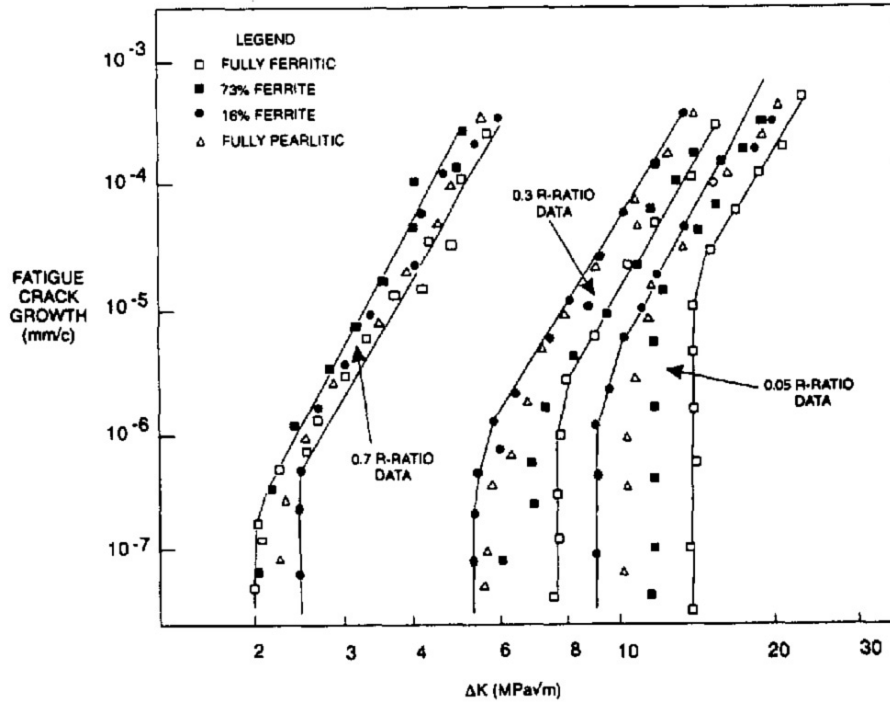


Figure 8: Fatigue crack growth for different R -ratios and microstructure [14].

From the values Bulloch found in his study (shown in figure 8) he constructed three sets of constants used in Paris' law for different R -ratios ($\frac{da}{dN}$ given in m/cycle and ΔK_I is given in $\text{MPa}\sqrt{\text{m}}$):

$$\begin{aligned} \frac{da}{dN} &= 6.12 \cdot 10^{-16} (\Delta K_I)^{6.7} & R &= 0.05 \\ \frac{da}{dN} &= 1.35 \cdot 10^{-14} (\Delta K_I)^{6.2} & R &= 0.30 \\ \frac{da}{dN} &= 2.59 \cdot 10^{-12} (\Delta K_I)^{6.5} & R &= 0.70 \end{aligned} \quad (7)$$

Bulloch also tries to make some statements considering the lowest stress intensity at which crack growth will occur, the threshold value $K_{I,th}$. The threshold is also seen in figure 8 as the point on the curves where the linear part in the log-log plot does not apply anymore

for the lowest values. The threshold values is defined as the stress when the crack growth is below 10^{-7} mm/cycle and it shows dependence on both R -ratio and the pearlite/ferrite composition (at least for low R -ratios). Bulloch makes an extrapolation of the threshold value to $R = 0$ with help from the three R -ratios used earlier. The threshold values for different R -ratios is shown in table 2.

R	0 %ferrite MPa \sqrt{m}	16 %ferrite MPa \sqrt{m}	73 %ferrite MPa \sqrt{m}	100 %ferrite MPa \sqrt{m}
0	11.3	9.7	12.7	14.5
0.05	10.2	9.1	11.8	14.3
0.30	5.2	5.8	6.5	7.5
0.70	2.2	2.2	1.8	1.9

Table 2: The fracture toughness threshold value $K_{I,th}$ for different compositions and R -ratios.

3.3 Overloading

When a crack is loaded cyclically with constant stress intensity amplitude, an exposure to a single amplitude peak will decrease the crack growth during subsequent cycles. This phenomenon is a result of the plastic zone occurring around the crack tip. The higher peak load creates a plastic zone with a greater radius than the one occurring during normal load amplitude. The plastic zone impedes crack growth through compressive residual stresses near the crack tip. A sketch of the overlapping plastic zones immediately after the overload is shown in figure 9.

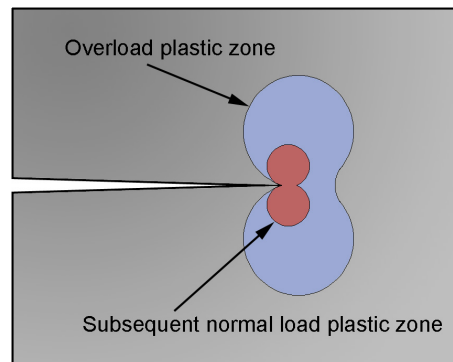


Figure 9: The plastic zones immediately after overload.

The frequency of overloads is critical because the effect will fade out after a number of cycles at normal load. On the other hand overloading too often will create a faster crack

growth. There will be an optimal number of cycles after which a load peak shall be applied to minimize the crack growth. The behaviour of a crack loaded optimally and a crack loaded with too few load peaks is shown in figure 10.

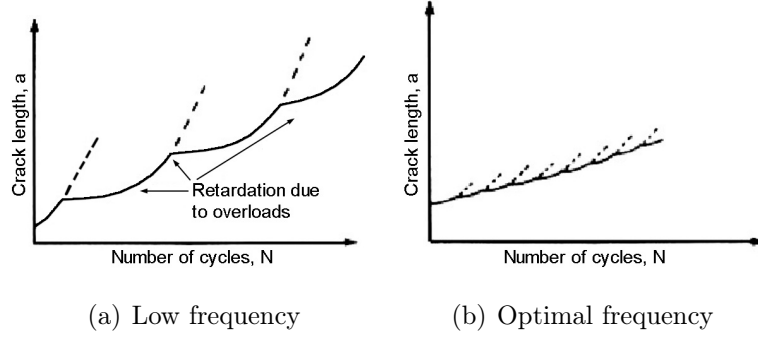


Figure 10: The effect of the overloading frequency on the crack growth [15].

There are a number of different models which describes the behaviour of a crack under differing loads; one of the most widely used is the Wheeler model. The Wheeler model includes the sizes of the plastic zones, both the overload zone and the normal load zone, and creates this way an estimate of how the crack growth is affected by the overload. The model predicts that the crack growth retardation is:

$$\left(\frac{da}{dN}\right)_R = \left(\frac{\beta\pi \Delta a \sigma_y^2 + K_o^2}{K^2}\right)^\gamma \frac{da}{dN} \quad (8)$$

K_o is the stress intensity at overload, β is a factor describing the stress state which is 6 for plain strain and 2 for plane stress and Δa is the crack growth since the overload. Even if the model is one of the simplest available it includes a fitting parameter, γ , which makes experiments necessary for different materials, load situations and environments. The need for experimental values makes the usage of the model limited to special situations, and the common way to treat problems including varying load is to approximate it as constant. Load amplitude peaks are retardation effects and neglecting them when calculating the lifetime is conservative [4] (pages 534-536).

3.4 ANSYS cast iron material model

The most striking property of the cast iron is the differing behaviour in tension and compression, this is essential to reflect in the material model. The cast iron does not have a distinct yield point and the modulus of elasticity shows a great extent of nonlinearity. Much

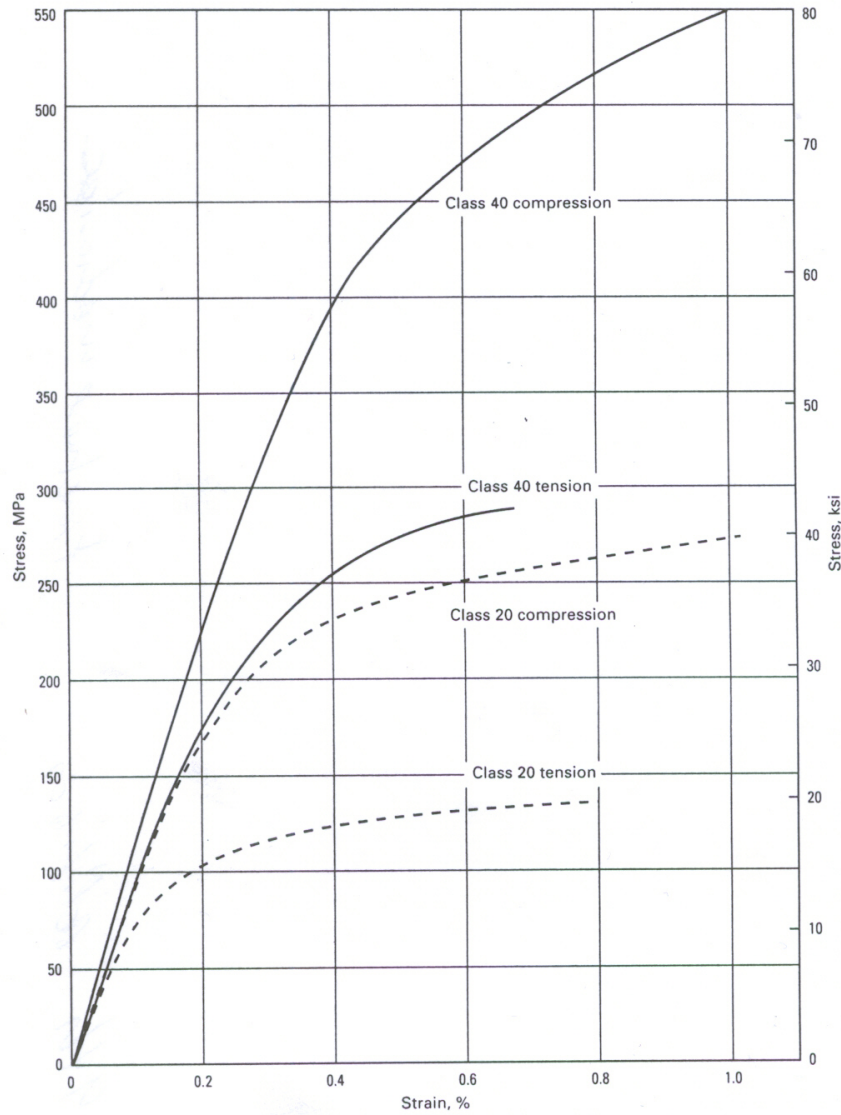


Figure 11: Load curve for grey cast iron [16]. The GG15HC iron has a little lower strength than the class 20 iron.

of the load curve shows in fact plasticity because the deformation under elastic premises only occurs at small strains, see figure 11.

The ANSYS material model of cast iron uses a yield criterion which is a combination of a von Mises cylinder:

$$\sqrt{3J_2} - \sigma_{y0} = 0; \quad J = \frac{1}{2}s_{ij}s_{ji}$$

and a Rankine cube defined by:

$$\sigma_1 - \sigma_{y0}; \quad \sigma_1 \geq \sigma_2 \geq \sigma_3$$

where s_{ij} is the deviatoric stresses, σ_i is the principal stress i and σ_{y0} is the (uniaxial) yield strength. This way the von Mises criterion is used in compression and the Rankine criterion is used in tension, a composite yield surface. This is shown in figure 12.

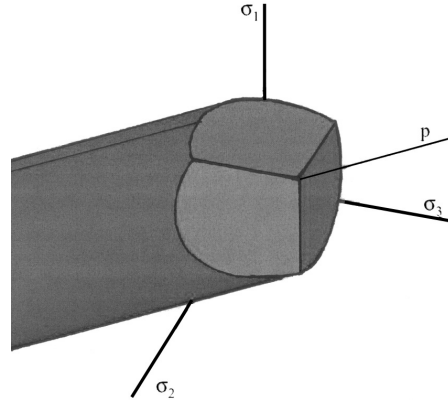


Figure 12: Principal stress space when von Mises' and Rankine's yield criteria are combined.

The yield criterion reflects the compression/tension dependence in yield of the material. The yield surface also takes the hydrostatic pressure into account. When loaded in compression the hydrostatic pressure does not matter due to the von Mises yield criterion. If the load changes sign and becomes a tensile one the hydrostatic pressure is considered by the Rankine criterion.

The elastic Poisson's ratio, ν , is input as a single value in the material model. The plastic Poisson's ratio in tension, ν_{pl} , is allowed to vary with temperature, but not with stress. In reality the Poisson's ratio has a dependence on load rate, but the model with two different values reflects the real behaviour rather well. The case is the same in compression but here the plastic Poisson's ratio is predefined as 0.5 due to the incompressible plastic behaviour of the material [17, 2].

The flow potential decides the direction of the incremental plastic strains when plasticity occurs in a body. The general flow rule can be written as:

$$\dot{\epsilon}_{ij}^p = \dot{\lambda} \frac{\partial g}{\partial \sigma_{ij}}$$

Where g is the flow potential and λ is a non zero scalar. The ANSYS model includes non associated flow, this is a property which is used for rocks, concrete and soil normally. The

graphite flakes in cast iron makes it behave in a similar way and less like steel and other metals. Associated flow means that the flow potential, g , is the same as the yield criterion, f . The non associated flow means that $f \neq g$. The flow potential is shown in figure 13.

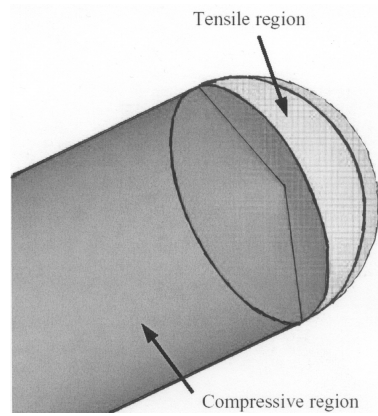


Figure 13: Flow potential in the ANSYS cast iron model [2].

Plastic incompressibility can be written as

$$\dot{\epsilon}_{kk}^p = 0$$

This is obtained for:

$$\frac{\partial g}{\partial \sigma_{ii}} = 0$$

When plastic incompressibility is included in the material model the invariant

$$I_1 = \sigma_{ii}$$

is included in the flow potential, this is not the case when there is no plastic incompressibility.

The material response in the model is nonlinear and the stress-strain curve used by ANSYS is multi linear, this is input by strain values and their corresponding stress values. There are two different tables; one considering the plastic deformation in compression and one considering the plastic deformation in tension. This is an important feature of the material model for cast iron because of the great difference in material response between compression and tension [2, 18] (pages 219, 227, 239-240).

The parameters used in the material model are described in appendix A.

3.5 Plastic shakedown

The stress-strain curve for cast iron is not suitable to be approximated with a linear model, a constant Young's modulus, E . This statement is only true under the circumstances in which the curve has been constructed; this is usually the first uploading with a certain load (in most tests uniaxial tension or compression). Figure 14 is showing repeated loadings of grey cast iron in tension. Also seen in the figure are the different paths which are followed when loading and unloading the material.

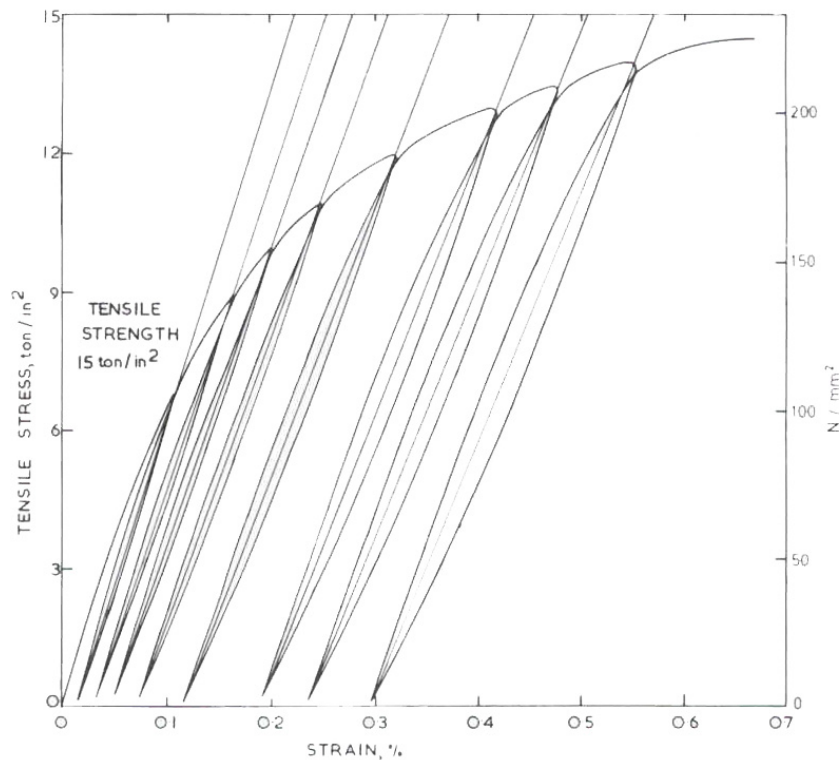


Figure 14: stress-strain curve when cast iron is loaded and unloaded repeatedly in tension to increasing stress levels. Before loading the iron was in *as cast condition* [17].

When the cast iron is loaded to a new stress level the behaviour shows a lot of nonlinearity. When loaded uniaxially to a certain stress level however, subsequent loading can be approximated as linear with a constant Young's modulus. This can be seen in figure 14 and is explicitly shown in figure 15. When problems in many dimensions are studied, the Young's modulus is substituted for the constitutive matrix D_{ijkl} as a relationship between stress and strain. For this matrix the same relations apply, and it also becomes constant after repeated loadings.

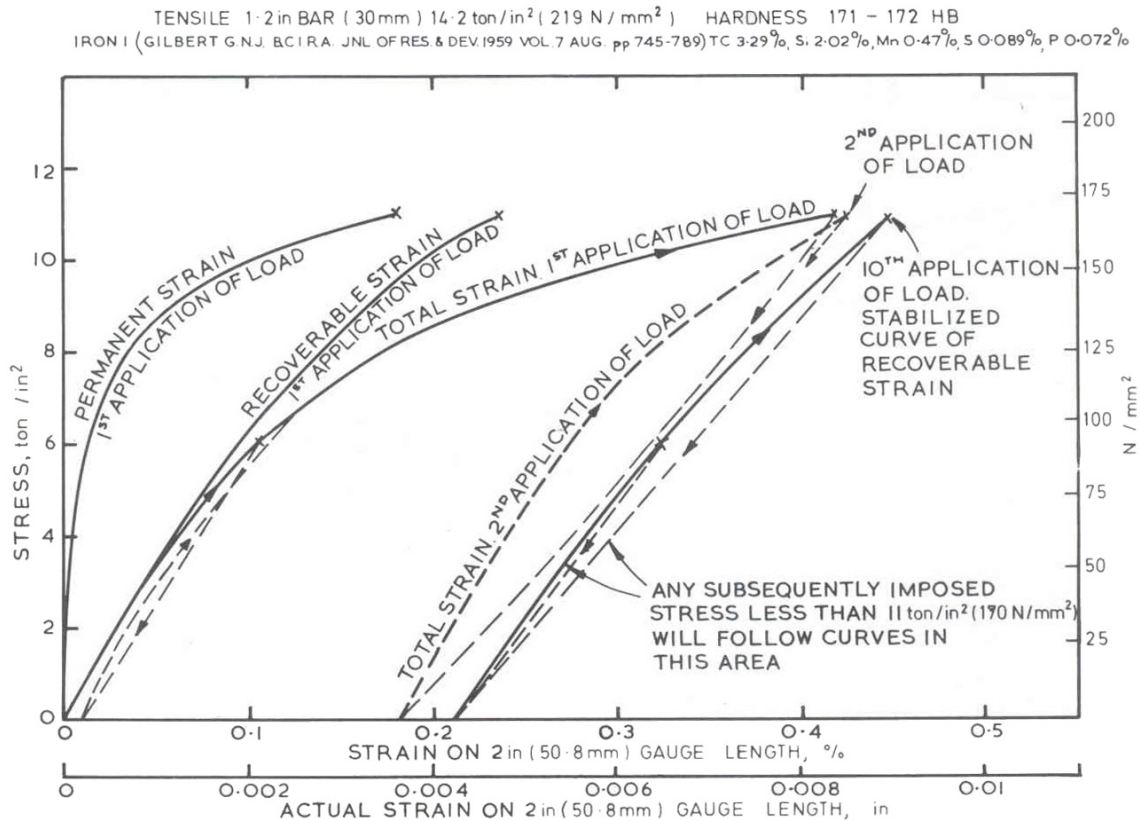


Figure 15: Stress–strain curve when cast iron is loaded and unloaded repeatedly, showing the elastic behaviour after some load cycles [17].

The linear behaviour of the cast iron in subsequent loading can be used with favour when crack growth is studied. When the interest is in growth of a crack the first loading of the material is not the most important, it is the repeated loadings after the first which makes the crack grow. Given the demand for a linear material model to make it possible to use linear fracture mechanics makes the choice to use the plastic shakedown theory easy.

One thing that makes the first loading interesting are the permanent deformations and the residual stresses which results from these deformations. These are parameters that shall be transferred to following loadings to achieve good calculation results [17].

4 Modelling

4.1 First simplified model

The first model of the disc is a cylinder clear from splines, the model cover $\frac{1}{120}$ of the entire disc using symmetry. This means six degrees in the circumferential direction and half of the disc thickness. A smaller part of the disc could possibly be used but the six degree measure is the one which has to be used in the more detailed model including the spline to cover the entire disc geometry. The simplified model is shown in figure 16(a). The disc in the model has an outer diameter of 390 mm, an inner diameter of 128 mm and a thickness of 20 mm.

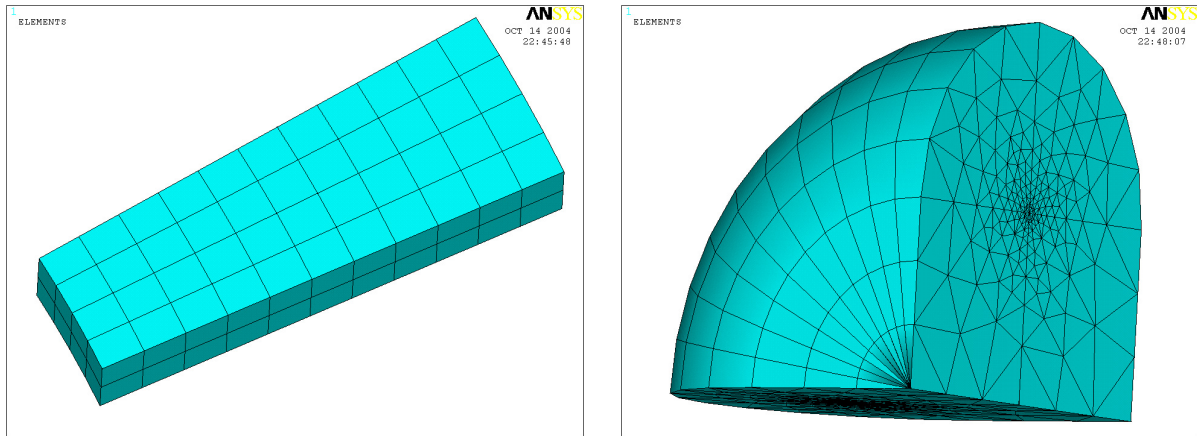
At the inner radius of this simplified disc model a half circular crack is placed (only half the crack is modelled due to symmetry giving quarter of a circle), the crack radius is three millimetres. To get a refined mesh around the crack, submodelling of a small portion of material in the vicinity of the crack is used. Using submodelling is based on St. Venant's principle which states that material far enough from a stress concentration is not affected by it. This way of working makes it possible to not model any crack in the full circular section shaped model, the crack only exists in the submodel. The submodel is placed at the same coordinates as the inner surface and the symmetry surface in the middle of the disc. This is a worst case scenario when placed in the middle of the disc the crack is loaded under plane strain conditions. The increased stress concentration is due to the transverse contraction strain which is occurring in the z-axes direction in the local crack tip coordinate system (see figure 5). This strain makes the stress concentration near the crack tip more emphasized.

Due to problems with convergence in the solution (probably because of a software error in ANSYS) only the stress-strain curve for 50°C is used in the simplified model. At all other points the model applies to the one defined in appendix A.

Loads

The first step in the calculations is to apply the heat load, this is done in a thermal analysis where the created effect is applied as a heat flux where 95% of the braking energy is assumed to go in to the discs as heat and the five remaining percents goes in to the pads. A worst case scenario where 55% of the braking is concentrated to one of the discs of the pair is used. The heat load is applied in four different ways; this approach is taken due to the banded heating of the discs which has been seen in practical tests:

The first way to apply the load is called case 0 and is the same one which has been used in previous calculations made at Haldex [19, 20] with all of the heat load applied outside the mean radius of the disc.



(a) Disc model

(b) Submodel

Figure 16: The simplified disc model and the submodelling of the crack.

The second to fourth way to apply the heat load is called case 1, 2 and 3 where the heat load is divided into two parts, one of them is applied to the entire disc side and the other is applied to a band that has a thickness that is one third of the radial distance between the inner and the outer radius. This band is placed along the inner radius in case 1, in the middle of the disc in case 2 and along the outer radius in case 3. The different load cases are visualised in figure 17. In the figures a section of the disc perpendicular to the tangential direction is shown, and the heat flux is plotted as boxes.

Convection and radiation at all free surfaces is assumed with a combination of the convection coefficient and the radiation varying according to figure 18(a) [1]. Air with a temperature of 20°C is assumed far away from the disc. At the interface with the hub the convection/radiation is assumed to be ten times greater due to the higher conductivity of the iron in the hub than in the surrounding air.

The load used is the one from a truck going down an 8% slope at a constant speed of 85 km/h with an axle load of 12200 kg with air and rolling resistance omitted. The load is ramped for 0.5 seconds at the beginning of the braking and then held for 40 seconds. After this braking a temperature field is created in the disc, this field is used in the structural analysis of the disc.

In the structural analysis the temperature field at 40 seconds was extrapolated over the disc as a body load to make it possible to use another mesh than the one used in the thermal analysis. This body load was ramped up from the bulk temperature in the disc at 50°C to the actual temperature field at 40 seconds. This is an assumption since the real temperature field in the disc does not vary linearly with time this way; the error made

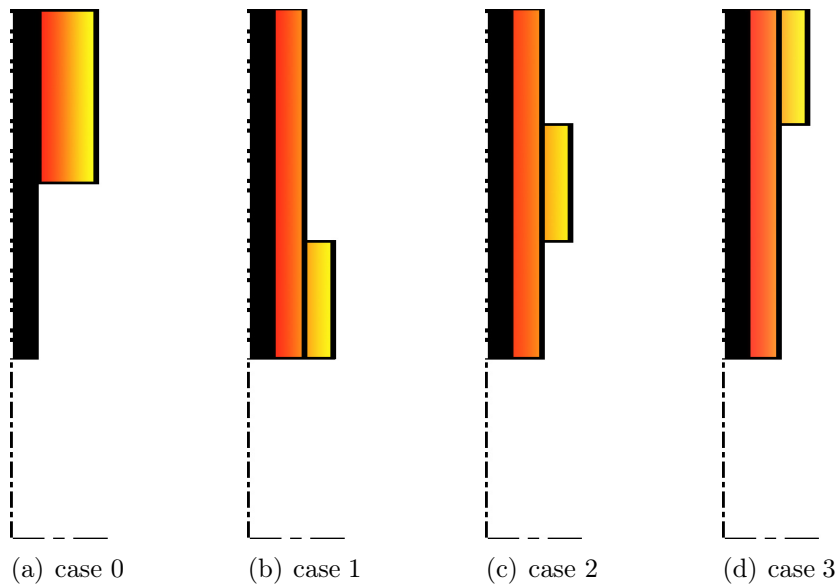


Figure 17: The different load cases used in the calculations on the simple model.

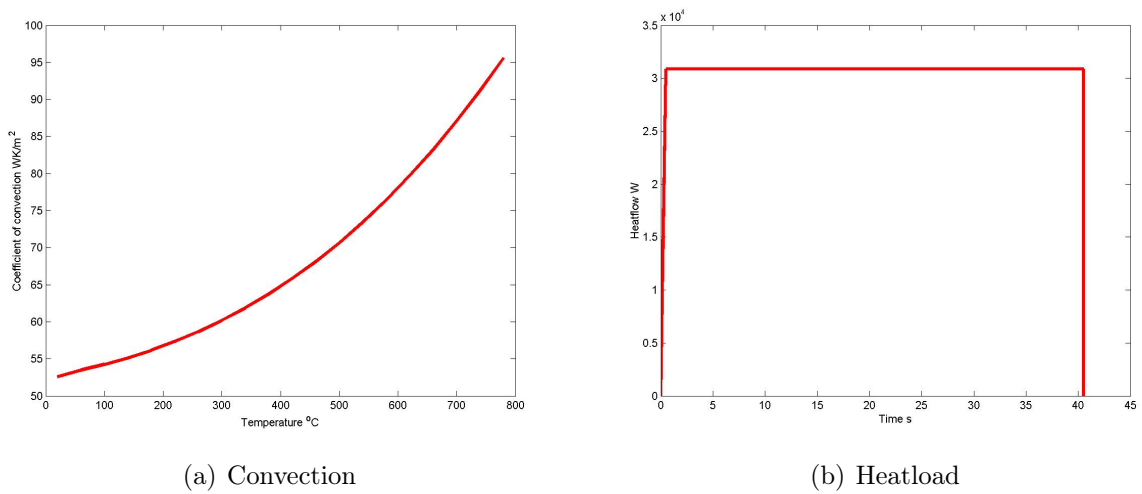


Figure 18: The heatload and the modified Convection coefficient.

is anyway marginal when loading the disc. This is shown in earlier calculations made at Altair and Haldex [21].

Meshing

When using linear fracture mechanics in finite element formulation use of elements with a quadratic formulation (elements with midside nodes) is necessary. Midside nodes in the elements around the crack tip shall be moved to quarter points, that is to say a point $\frac{1}{4}$ of the element length from the crack front instead of the midside of the element. This way singular elements are created reflecting the stress singularity $\frac{1}{\sqrt{r}}$ around the crack front. The singularity of the elements arises from the formulation of the quadratic isoparametric elements where the shape functions show this behaviour when the nodes are placed at quarter points. Figure 19 shows elements modified to surround the crack tip [4] (pages 586, 595-598).

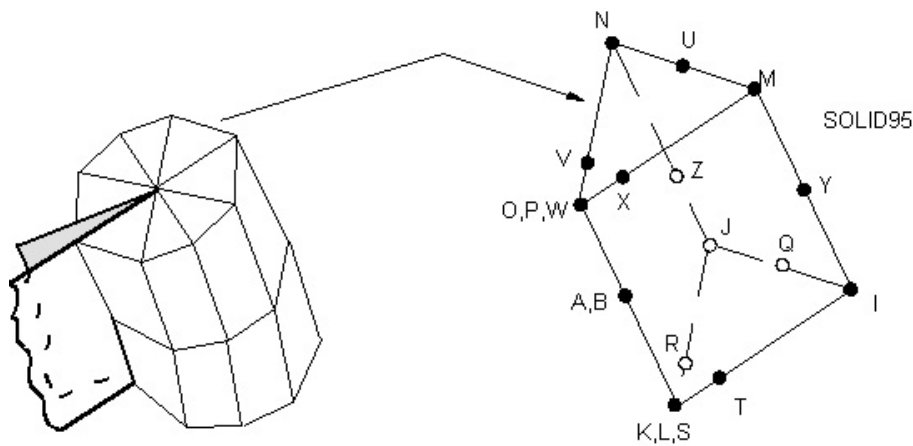


Figure 19: Elements modified to surround the crack tip [9].

ANSYS have commands to create singular elements around a crack tip in two dimensions (plane stress/plane strain simulations) called KSCON, this command does not work in three dimensions. To model a three dimensional crack you can build the model placing the nodes first and then creating the mesh by hand or by some kind of looping. Another way is to use a trick making it possible to use the KSCON command; namely meshing one of the surfaces of the body with special "mesh only" elements – elements only used to create a mesh but with no calculation possibilities. In ANSYS these elements are called MESH200. The advantage with "mesh only" elements is that they can change dimension when extruding an area to a volume. The extrusion in this case is done along a curved line representing the crack front, a *drag path*. Creating a three dimensional mesh this way gives brick elements, elements collapsed into wedge elements or non collapsed wedge elements, depending on method, all over the body. To pick up the steep stress gradient near the crack front the nodes is concentrated in the vicinity of this line through the submodel. The major

disadvantage with the method is that the KSCON command requires free meshing of the surface used in the drag operation. The free meshing makes the control over the mesh appearance limited. This method used to create a three dimensional finite element crack model is proposed by X.M. Jia and F. Dai [22].

The geometry of the disc model makes some moving of nodes after the creation of the three dimensional submodel necessary. This is due to the curved inner surface of the disc and the fact that it is not possible to create elements along a drag path with zero length like the one created in the corner between the inner surface of the disc and the symmetry plane. The submodel is shown in figure 16(b).

The structural analysis is made with ANSYS cast iron model (see chapter 3.4) with the material parameters shown in appendix A. It shall again be remarked that only the stress-strain curve for 50°C is used.

Submodel

When the structural analysis is solved the displacement field for the entire body is known. This field is interpolated over the surface nodes at the submodel. The displacements are used as boundary conditions when solving the submodel with the crack. If the boundary is far enough from the crack face, the solution of the submodel will approach the exact solution. The temperature field from the full model is also interpolated over all the submodel nodes. In order to use linear fracture mechanics the material properties must be approximated as linear. This is the reason why the ANSYS cast iron model is not used in favour of a linear model with a constant Young's modulus. Solving the submodel gives a new displacement field around the crack. With this field it is possible to calculate the stress intensity factor, K_I . This is done with the approximating method using the displacement of the nodes at the crack face near the crack tip described in chapter 2.1.

Results

When loaded for 40 seconds the temperature gradients in the disc are maximized, this gives the biggest strains and hence the largest stress intensity values.

The stress intensity values from the calculations are shown in table 3. Both values when the disc has maximum temperature and temperature gradient at 40 seconds, $K_{I,warm}$, and values when the disc is cooled down to 50°C after loading, $K_{I,cooled}$, are shown. Values are measured at three places along the crack front, at the inner surface of the disc, at 45° along the crack front and in the middle of the disc at the symmetry surface. At the inner surface, plane stress condition is assumed when calculating the stress intensity factor. At the two remaining points, plane strain conditions are assumed.

	inner surface		at 45°		symmetry surface	
	$K_{I,warm}$	$K_{I,cooled}$	$K_{I,warm}$	$K_{I,cooled}$	$K_{I,warm}$	$K_{I,cooled}$
case 0	19.78	5.40	21.85	7.74	21.72	7.75
case 1	9.58	1.93	9.10	2.16	8.90	2.15
case 2	5.28	0.42	5.32	0.61	5.24	0.61
case 3	12.40	1.86	11.64	2.91	12.48	2.92

Table 3: The resulting values from the crack tip analysis values in $\text{MPa}\sqrt{\text{m}}$.

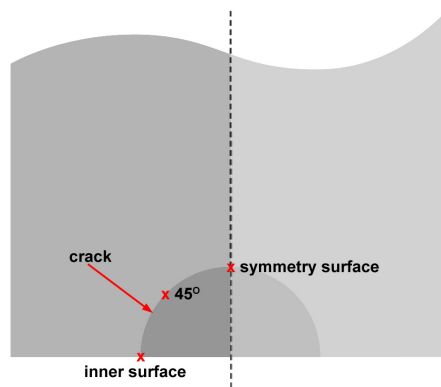


Figure 20: A cut in the radial–axial plane through the disc, showing the points where stress intensity values are measured.

4.2 Second model

The second model used has the real geometry of the Wave Spline discs, earlier described in chapter 1.3. This disc has the outer radius 390 mm and the thickness 20 mm. The element mesh for the entire disc model was created by M. Wallin [21]. In this entire disc model the use of symmetry is maximized, making it possible to only look at $\frac{1}{120}$ of the disc. Wallin also delivered results containing stresses, displacements and temperature field for a disc during the first loading, a cooled disc and a disc during the second loading. Wallin used the load case 0 described in chapter 4.1 but without any influence from radiation. The real temperature field was used in structural loading of the discs. Then the temperature field was ramped linearly when unloading in the structural calculations.

The material model used is the one in appendix A with three stress-strain curves for different temperatures. The material stiffness is determined with an interpolation between these curves for the actual temperature in a point.

The calculations concerning crack growth are made like in the preceding chapter with submodelling. The arguments for this methodology are the same as earlier. In this case

however, the geometry of the spline makes the presence of cracks in certain points more probable than others. Indications of this are seen in calculations foregoing these as a concentration of plastic strain in these points. When modelling, the points with maximum principal plastic strain are chosen as they are the natural placement of a crack. This gives the placement for the submodel because it surrounds the crack. The principal plastic strain distribution is shown in figure 21.

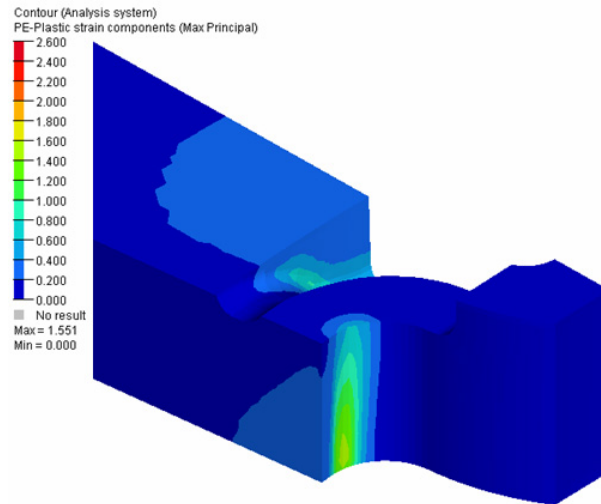


Figure 21: The maximal principal plastic strain distribution in the cog region after 40 seconds of the first loading [20].

The orientation of the crack is not as evident as the placement, not in the initiation phase anyway. Later on when the crack has grown to a certain length it is obvious that the growth is mainly in the radial direction. This is the reason why the modelled crack is oriented as a radial line from the centre of the disc towards the periphery passing the most affected point.

Loads

The axle load used in the calculations is 12200 kg. The loading is the same as in the preceding model, representing a truck going down a slope at 85 km/h with a constant retardation of 0.82 m/s^2 (this corresponds to a slope of about 8% with the air and rolling resistance neglected). The time, the load applied and the assumptions about how much of the effect that goes in to the disc are the same as in the first model, and this is described in figure 18(b) and chapter 4.1. The temperatures used are also the same as in preceding chapters.

Meshing

With the disc model and all the results taken from calculations made by Wallin the modelling is concentrated to the submodel.

The meshing of the submodel follows the one in chapter 4.1 to great extent, but the spline geometry makes it harder to create the submodel. The geometry of the inner disc surface has to be reflected in the submodel, this is because of the free surface necessary for the crack to open. At all the other surfaces the displacements are prescribed through the submodelling process. The use of the KSCON and VDRAG commands described earlier creates borders for the modelling. Problems occurring are mostly ungluing of the mesh or the volumes building up the model. Creating a small gap between the crack faces makes it easier to get rid of problems with gluing of nodes. These problems occurred when giving the crack faces the same coordinates. The crack tip is of course modelled by only one node in the plane. The drag path have straight lines in the both ends, this is also due to problems to get the areas sticking together, this way the crack front is not a perfect quarter of a circle but the disagreement is very small.

The inner surface can not be modelled by just moving the nodes like in the simplified model; the reason is the smaller radius in the spline in comparison to the inner radius of the entire disc. This makes it necessary to create volumes between the ones created in the drag operation along the crack front, and the inner disc surface. These volumes are also created in an extrusion operation of areas at the symmetry surface in the middle of the disc. The areas are built up by points at the inner edge of the disc connected by a B-spline curve and straight lines. These transition volumes have not got modified elements in the crack tip, this means that they do not reflect the stress concentration at the crack tip. The stress concentration at the free surface is not very interesting anyway, for reasons given in earlier chapters. The problems with the lack in reflecting the real behaviour of the metal at the inner surface shall not affect the model a small distance from this point along the crack front. The submodel and the placement of it is shown in figure 22.

Solution schedule

To make the calculation model reflect the plastic shakedown, a solution in many steps is employed. To be able to use values from earlier calculations the entire disc model used earlier was imported. These earlier calculations were made by Wallin in ABAQUS and to use the results in ANSYS the model has to be transferred between the two programs. This is done with text files using the same kind of commands (APDL) as in the input files used to control ANSYS normally. Not only already derived values were deployed. Wallin also made new calculations obtaining values for a cooled disc. This was done to obtain plastic deformations and residual stresses originating from the heat load. The calculations in the submodelling procedure are made in the following steps:

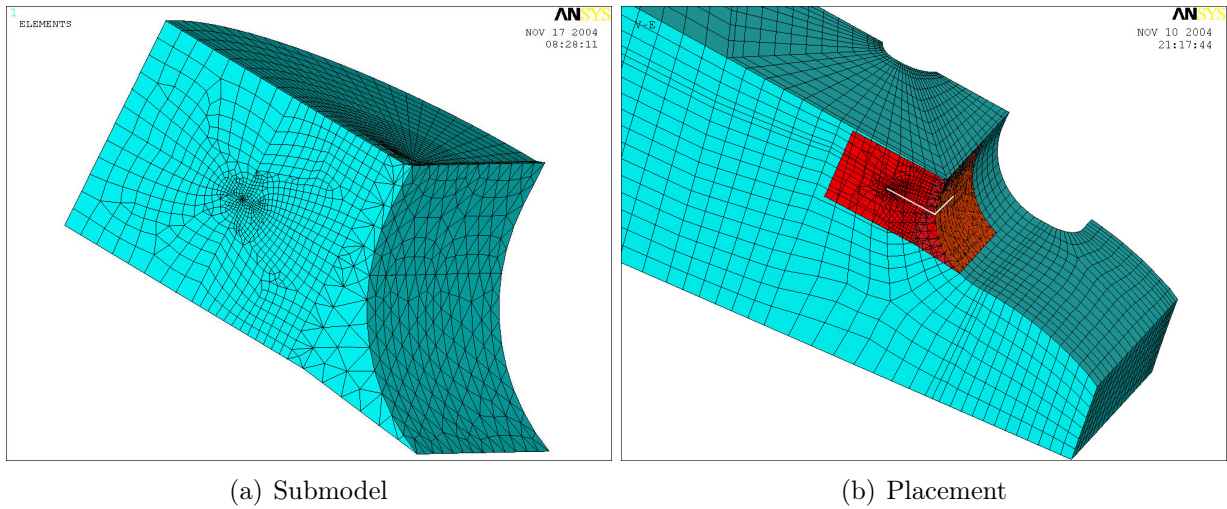


Figure 22: The submodel and the placement of it in the disc. The image of the placement is just made to show how the submodel is placed, when making the calculations the submodel is totally free from the full model.

- Creating a full model of the brake disc (using symmetry of course). In this case the full model is imported from ABAQUS.
- Creating a submodel and giving it boundary conditions such as symmetry.
- Making a thermal load cycling at the full disc model, here only the loading of the disc is made, and not the cooling.
- Use the temperature field when the temperature/thermal gradient is maximal in a structural analysis (this happens just before the heat load is removed in the studied problem). Ramping the temperature first up, then down again to the initial condition, creating plastic deformations and residual stresses in the disc. This step and the preceding are done in ABAQUS and the value are then imported to ANSYS.
- Transferring plastic deformations to the submodel from the entire disc model. "Resetting" the submodel in this condition, making the plastic deformations permanent and the submodel stress free.
- Transferring the residual stress field from the entire model to the submodel.
- Making a second loading of the entire disc model with the temperature field derived earlier used in a structural calculation. This is also done in ABAQUS.
- Transferring the temperature field to the submodel and using the displacements derived in the second loading at the boundary nodes of the submodel.

- Solving the submodel with the temperature field, the residual stresses and the displacements at the boundary applied.
- Post processing the solved model using the method described in chapter 2.1 to derive the crack intensity factor, K .

Export and import

The temperature field is imported as initial conditions because this does not change when solving the structural problem. To use the values for submodelling or post processing it is necessary for ANSYS to read them from a result file. To create such a file a solution has to be done. With the problems described earlier with the material model for cast iron, the result file has to be altered after the creation with a simplified material model. The right displacements and the stresses are transferred this way and written to the result file. Both the displacements and the stresses are written to the nodal points. For the displacements this is no problem, displacements are derived in the nodal points. For the stresses on the other hand extrapolation of the values in the integration points to the nodes has to be done before writing them to the result file.

Between the full model and the submodel transfer is carried out by commands that interpolates the temperature field and the displacements between different element meshes. The command used for interpolating the temperature field is called BFINT and the one used to interpolate the displacements is called CBDOF. For the stresses no such command is available. Thus the stresses are transferred using a trick.

The command used to plot results in graphs is called PATH, with this command arbitrary points in the model are defined and ordered along a *path*. When a path is defined, different results can be mapped to it for later use, creating for example curves in a graph. The points are arbitrarily placed in the model; this makes it necessary for the program to interpolate values from the nodes or the integration points to the points at the path. It is the interpolation of the results made by the PATH command which is used when transferring stresses to the submodel. The transfer is made according to:

- A path is defined in the full model with the path points placed at the coordinates of the submodel element centroids in the global coordinate system.
- Stresses in all directions are mapped to the path points and thereby an interpolation is made from the integration points to the position of the submodel element centroids.
- The stresses are written to an initial stress file to be used with the ISFILE command.
- The submodel is loaded in to the program and all constraints are set, in the solution processor the ISFILE command is used before solving the problem prestressing the model with the residual stresses from the preceding loading.

Results

	at 45° K_I MPa $\sqrt{\text{m}}$	symmetry surface K_I MPa $\sqrt{\text{m}}$
radial crack warm	19.79	20.24
radial crack cold	7.29	7.47
radial crack warm 4 mm	17.22	17.03
radial crack refined mesh	20.27	20.39
crack perpendicular to spline	19.45	17.94
relocated crack	20.08	21.44

Table 4: The resulting values from the crack tip analysis.

The resulting K_I stress intensity factor values are shown in table 4, in the table both values for the disc with the maximum temperature and the cooled disc are shown. The table also includes values for a submodel with a crack oriented perpendicular to the spline fillet, a submodel with a crack radius of 4 mm and a submodel that has been placed at a slightly different location for comparison. The relocated submodel is displaced by approximately 1 mm in the tangential direction. To verify that the mesh size is small enough, a submodel with a refined mesh is made, in this model the number of nodes is increased from 50527 to 98841 and the resulting values from this model is also included in the table. The difference in crack intensity value K_I between this and the other radial crack model is an increase with 0.7% for the refined mesh. The minor difference between this and the other radial crack model confirms that the mesh size in the model is not too coarse or that the result is destroyed by deformed elements.

When calculating the stress intensity factor, a plain strain condition is assumed, this is done both in the middle of the submodel at 45° along the crack front, and at the symmetry surface of the model. The assumption of the plain strain condition is conservative because κ (see equation (5)) will always be smaller under plain strain than under plain stress, and hence the stress intensity factor, K , will be greater.

To make use of Paris' law with the parameters given by Bulloch in equation (7) the difference in stress intensity, ΔK_I , and the R -ratio has to be determined. This is done for values originating from the symmetry surface, and the resulting values are:

$$\Delta K_I = 12.77 \text{ MPa}\sqrt{\text{m}} \quad R = 0.3691$$

If figure 8 is studied it is seen that this tangents the border of the measured values Bulloch presents. This is mainly because his aim is to describe crack growth near threshold values.

A linear interpolation between two of the equations (7) gives new parameters for the R -ratio in the current case:

$$\frac{da}{dN} = 4.58 \cdot 10^{-13} (\Delta K_I)^{6.25}$$

If ΔK_I is inserted into this equality this gives a value of $3.77 \mu\text{m}/\text{cycle}$ for the crack growth.

Only the factor K_I is considered above, but the calculations also shows that the crack to some extent is loaded in mode II (see figure 4). The influence from this loading is only about $\frac{1}{10}$ of the value for mode I. This is a result of the orientation of the crack, if the crack is oriented radially the K_{II} -factor is decreasing and the K_I -factor is increasing compared to the crack oriented perpendicular to the spline fillet. This proves that the crack growth is mainly near the radial direction in the discs. The major crack growth will be in the direction where K_I is maximized if no material inhomogeneities are present. The presence of K_{II} loading in the case with the radial crack shows that the K_I value might be a little higher if the crack has a slightly different orientation. There are methods used to combine intensity factors (see [23]) to create an effective stress intensity factor, K_{eff} , but none of these methods are well established or used in normal practice. Therefore a careful use of the K_I stress intensity value is used in favour of such methods, and the value of K_{II} is only used as an indication of the crack orientation.

The orientation of the crack is probably the explanation to the somewhat surprising values for the relocated crack; the stress intensity is increased compared to the crack placed in the most affected point of the spline. A study of the K_{II} values for the both configurations shows that the relocated crack has a great decrease in stress intensity in this mode. The value of $2.2 \text{ MPa}\sqrt{\text{m}}$ for the original crack has decreased to $0.2 \text{ MPa}\sqrt{\text{m}}$ for the relocated crack. At the same time the relocation is small so that the crack is hardly moved out of the most affected zone, this further explains the relatively high values for this model.

The results for the submodel with a 4 mm crack radius show that there is a slight decrease in the crack intensity compared to the model with a 3 mm crack. The decrease in stress intensity can be a consequence of the crack growing out of the most affected section of the disc. It is evident that the decrease in stress intensity does not originate from unfulfilled conditions for submodelling. This is seen in studies of the displacement field and the stress field of the submodel, where the gradients would be steep if the conditions were not fulfilled. The conclusion to be made from this is that the crack growth rate can be assumed to be quite constant at values of the crack radius in the vicinity of 3 mm.

Usage of equation (3) with the crack radius 3 mm, the calculated growth rate and the value of n gives an approximated service life for the disc until its total failure. The number of cycles which the disc will survive is 338 according to this method. If the growth rate instead is assumed to be constant with a crack length in the vicinity of 3 mm the results differs some. That the growth rate is constant under these premises is shown to be probable

by the 4 mm crack model. If the crack is assumed to grow at constant rate from 3 until 4 mm, this growth will require 265 load cycles. If equation (2) is used instead to predict the number of cycles this gives the result 171 loadings.

5 Discussion

The interpolation of values which is made when importing and exporting between ANSYS and ABAQUS, gives some loss in exactness. This problem primarily occurs when transferring the stresses to the submodel. The stresses have to be written to each node from the integration points in ABAQUS, and the stresses then have to be interpolated to the nodes of the submodel in ANSYS. Temperatures and displacements do not have to be interpolated more than once; from the full model to the submodel as part of the normal submodelling.

To be sure that the studied crack placement really is a worst case, other crack placements, crack lengths and crack orientations might be interesting to study. This is done with a number of different models but additional modelling can increase the knowledge. To place a crack arbitrary is however not a good way to deal with the problem. To do it effective it is better to structure the work as proposed in chapter 6.1. To answer the question about when the total break down of the structure happen, a macro crack in the full model would be necessary. Even different heat load cases might be interesting to study, even when the simplified model has pointed out that the load case used is among the worst which is probable to occur. It is even possible that the load case creates a heat distribution worse than any existing in reality. The most common heat distribution in real discs is with the major heat input close to the hub due to the higher pressure from the pads here (close to case 1 in chapter 4.1) [25]. With more different load cases it would be possible to make a more realistic life time estimate – less conservative.

Even though the thermal load has, by far, more influence on the plasticity in the discs and on the crack growth, some studies where the structural load is included might possibly lead to a better understanding of the problem. Including the structural loading can result in moving the most affected volume to a slightly different position. This is also the major deviation from the conservative approach used in all earlier calculations; it is possible that the structural load contributes to the crack growth. The thermal load is anyway the greatest source contributing to the crack growth, and the greatest problems originating from the structural loading are contact stresses in the spline.

No values are found for the critical stress intensity K_{Ic} considering grey cast iron, but as a comparison values for SG graphite iron can be used. At room temperature the critical stress intensity for this material is between 60 and 80 MPa $\sqrt{\text{m}}$ [26]. The corresponding values for grey cast iron are probably lower but this gives an indication about the magnitude. From this, a conclusion can be made that even if the values used earlier in the lifetime prediction tangents the border among the values measured, the equations most likely still applies. This can be understood from figure 6. It can also be seen that the requirement to make one able to use Paris' law ($K_{I,max} < 0.9K_{Ic}$) probably is fulfilled. That the other requirement regarding minimum load ($\Delta K_I > 1.1K_{I,th}$) is fulfilled can be seen from the values in table 2 where the values for 100% ferrite iron applies.

The crack growth values are derived from tests with CT specimens, and even if the K_I value is supposed to be independent of geometry, the usage considering surface cracks could result in some erroneous results. There are in fact methods used to translate the stress intensity from two dimensional plane strain values, to values considering the growth of surface cracks. The problem with these methods is that they anyway overestimate the growth, just like the use of plain stress approximation [24]. This and the lack of well established methods are the reasons that these kinds of equations are not used here.

Crack closure phenomenon are deviations from calculations connected to contact between the crack surfaces at low loads. Closure can originate from a number of sources: Plasticity, surface roughness influenced by the microstructure, oxides and fluid between the crack faces are things that can obstruct crack closure. Part of the problem with deviation in calculations is overcome by using the three equations considering different R -ratios. These differences between different load ratios improves the derived values since the crack closure is correlated to the difference between unloaded and loaded crack [4, 24] (pages 520-530).

A better knowledge about which material defects that can possibly occur, their geometry and changing of material characteristics originating from them, is another way to make better predictions considering the lifetime of the brake discs, and their risk of failure.

The integration of Paris' law (2) requires that the stress intensity is independent of the crack length; this is a doubtful simplification especially when the stress intensity value for the 4 mm crack is known to be the same or less than the one for the 3 mm crack. This assumption contributes to an overestimate of the crack growth. The big difference in the number of cycles required for the growth between 3 and 4 mm, depending on if an integration of Paris' law is used, or if constant growth rate is assumed, shows that the simplifications used when integrating Paris' law are not suitable in this situation. The geometry influence and the stress range are not constant during growth (f and σ in equation (1)). To clarify what approximations are used during the calculations, these are listed in table 5.

Conservative

- The heat load situation is probably worse than what occurs in reality.
- Varied load slow down crack growth through overload.
- Plane strain conditions are assumed.
- Values from CT-specimen are used for a surface crack.
- The load is not the same in every cycle, and the worst case load can not be repeated every time.
- Crack closure can impede crack growth.
- The crack will not grow straight in the radial direction in reality due to the inhomogeneous microstructure.
- When the crack grows out of the most affected zone the growth rate will decrease.
- Results are taken from the second loading, later loadings will create less plasticity.

Non conservative

- Only the heat load is included, not the structural.
- Only the load in mode I is included in calculations.
- Graphite flakes have a lower strength than the surrounding material.
- The crack growth rate is at the border among values from experiments [14].
- Difference in material properties between the disc material the one used to define material parameters.

Table 5: Conservative and non conservative approximations used in the calculations.

6 Improvements

6.1 Design criterion

The way to find the area most affected by the thermal–structural loading has recently been to find the maximum principal plastic strain, as described in chapter 1.3. This method gives a good indication on how the condition of the present design is compared to other, and an indication on where the most affected volume in the construction is to be found. However the method does not take the effect of repeated loading in to account, it is possible that the most plastically affected zones during the first load cycle might not be the same in subsequent loading.

Charkaluk, Thomas among others propose a refined method for locating the places where crack initiation is most probable in a thermally loaded body [27, 28]. To find the most probable place for a crack to origin, the energy dissipated per cycle is used as a damage indicator in their work. The energy dissipated per cycle, the *plastic strain energy density*, in an elastoviscoplastic material can be written as:

$$W = \int_t^{t+T} \sigma_{ij} d\epsilon_{ij}^p$$

Where ϵ_{ij}^p is the plastic strain. The integration is done over one cycle, this cycle is supposed to be taken when the material have found a steady state. The steady state behaviour is described earlier in chapter 3.5. Instead of approximating the material as linear elastic after a number of cycles as earlier, this method investigates the existence of points where plasticity occurs even after a number of load cycles. The mechanical energy dissipated in every load cycle is believed to play a part in the crack growth. The criticism that has been presented against this method is mainly that it is not known how much of the dissipated energy that contributes to the crack growth, and how much that is dissipated like heat. In the three articles [27, 28, 29] a lifetime estimation based on this energy called *the Morrow model* is used:

$$N_f^m W = C$$

Where m and C are material parameters and N_f is the number of cycles to failure. Hong et al [29] makes a comparison between the Morrow model, and the model called the *Coffin–Manson model* in which the energy W is substituted with the difference in plastic strain $\frac{\Delta\epsilon_p}{2}$ during one cycle. This model is essentially the same as the one used previously in the development of the Wave Spline (see chapter 1.3). Hong et al does not point out one method as superior to the other, this can have the explanation in that their study considered uniaxial tensile tests. The main advantage with the dissipated energy formulation is that

it can be generalized to the multiaxial situation [27]. The advantage of this method is also shown through good agreement between calculations and experiments made by Charkaluk, Thomas et al. This is interesting especially as they work on an area close to the one studied here – exhaust manifolds made of cast iron [27, 28].

Due to limitations in the ANSYS material model for cast iron (see chapter 3.4) cycled loading is not described in a good manner, this makes it necessary to look at the plastic strain energy density distribution after the first cycle. The result of this will in most cases be very close to the one derived when looking at the maximal principal plastic strain. With the plastic strain energy density as damage indicator the multiaxial behaviour of the loaded body is considered.

Even if the plastic strain energy density can be used in a lifetime estimate [27], this criterion is not proposed in favour of the more established relationship including K , described in Paris' law. This is mainly due to the possibility to find material parameters for grey cast iron. With this method an initial material defect is assumed and this is not any drawback in the situation.

When the volume most affected by plasticity is found by the methods above, a submodelling of this area with a modelled material defect is to be done. The material defect is preferably represented as a sharp crack, since this is a worst case scenario. The submodelling is with advantage made by the methods described in chapter 4.1 and 4.2, since this is the most convenient method found for creating crack tip elements in three dimensions.

The fact that the plastic strain energy density can be used to predict lifetime, as mentioned above, guarantee that looking at this energy gives a clear picture of the design status [27, 28]. The submodelling made throughout this work does not entirely point out the connection between maximum principal plastic strain affected areas and the crack growth rate. The connection is of course not direct, when it is possible for the crack to grow out of the most affected zone and the growth rate is thereby slowed down. But combined with the results by Charkaluk, Thomas among others it stands clear that this method can be used with good results to prevent the problem with cracks.

The goal with the design process is to create discs that do not collapse. To achieve this with a given crack growth some kind of instruction of maintenance probably has to be made. The way this was meant to be achieved before the results of this work were derived was a prescribed check of the disc surface every year. This kind of visual inspection can only detect cracks that are present in the surface of the disc and, as has been mentioned earlier, cracks inside the disc can grow faster. The cracks also have to grow to a certain length before they are discovered, and when this has happened there is a risk that the growth rate is too high for the discs to survive another year until the next service.

Instead another method has to be chosen; a crack originating from an initial defect is not allowed to grow to collapse length during the entire service life of the discs. This approach creates a schedule of requirements in accordance with table 6.

Initial defect size $< x$ mm	\Rightarrow	Crack growth $< y$ $\mu\text{m}/\text{cycle}$	\Rightarrow	Maximum number of cycles z	\Rightarrow	Maximum crack length $y \cdot z$
---------------------------------	---------------	--	---------------	---------------------------------	---------------	-------------------------------------

Table 6: Requirements on the design to avoid collapse.

The maximal size of an initial defect is believed to be approximately 3 mm as mentioned earlier. The service life of a truck is about 10^6 km. This creates requirements on the crack growth and thereby on the load and service intervals.

6.2 Improvements in design

A way that hopefully makes the strain distribution more even in the spline section of the disc is a small change in geometry. To broaden the inner wave pattern in the parts where material formally has been removed in order to give it the same width as the rest of the disc, can probably reduce the concentration of strain in these points. The problem with this change is possibly that it increases the risk of surface cracks, due to the stiffening of the inner part of the disc. There is also a risk that it will move the most affected points towards the disc surfaces in the axial direction. This would make the discs more sensitive to bending. The proposed changed geometry is shown in figure 23 this image is preferably compared to figure 3 at page 4. An equal change in geometry is to reduce the material in the tip of the teeth, creating an inner spline of equal width this way instead; this requires that the contact stresses from the structural loading will not increase too much.

6.3 Overloading

The behaviour of a crack zone described in chapter 3.3 can be used in order to impede crack growth. A prestress brake cycle can for example be prescribed before use of the brakes. Such a cycle should contain heating of the discs with steeper temperature gradient than the ones that will be created later during service of the brakes. Making this may perhaps slow down crack growth originating from material defects present at critical locations. The risk is of course that this treatment lengthens present cracks, but this might make it more probable to find defects. Another drawback is the fading out of the effect from the overloading as described in chapter 3.3. This effect makes the overloading methodology most effective if the overloading is repeated after a certain number of load cycles.

Before creating any routines considering pre treatment of this kind, experiments must be made to ensure that the treatment creates a more favourable situation postponing crack creation. The fitting parameter, γ , in the Wheeler equation ((8) in chapter 3.3) or similar



(a) Original geometry



(b) Changed geometry

Figure 23: The changed Wave Spline geometry.

parameters in other expressions is a first step to clarify if overloading the crack is a good way to hold back the crack growth.

As suggested above the overloading can be made like an imitation of a real brake cycle with the disc mounted in some kind of brake assembly. Other ways to create a favourable residual stress field in the disc might be to create thermal gradients in the disc by for example some kind of induction heating, or similar treatment. Methods more aimed at inhibiting the crack initiation rather than hold back an existing crack includes shot peening and cold rolling of the inner radius of the disc. These are methods connected to the overload methodology but affecting a larger section than just the critical points and create compressive residual stresses.

7 Summary and conclusions

7.1 Summary

The objective of this thesis was to create a way to avoid collapse of the Fixed Calliper Discs through cracks growing all the way from hub to periphery, a problem that has occurred earlier in prototype discs with other geometries.

The methods of calculating the number of cycles necessary for an initial defect to grow to a crack length that endanger the stability of the disc and makes a collapse likely, includes using a nonlinear material model coupled with a submodelling methodology. The usage of a submodel creates possibility to use a well established calculation technique including the linear stress intensity factor and Paris' law. The method is an attempt to imitate the real behaviour of the disc material which is believed to find a state of plastic shakedown, leave its nonlinear behaviour and adopt a linear, after subjected loadings.

When long cracks run the risk of growing fast the most promising way to prevent collapses of the studied type is found to include an instruction of how long the discs are allowed to be used rather than an instruction considering inspection of discs. This conclusion is based on the fact that dangerous cracks is not always seen at the disc surface but can be embedded in the middle of the disc.

7.2 Conclusions

The problems in using the integration of Paris' law (see chapter 5) makes the method of assuming a constant growth rate more fitting, especially as there are in fact signs showing that the growth rate might decrease when the crack leaves the most affected region of the disc (see also the calculations considering testing appendix B). This makes an estimation of the crack growth rate at $4 \mu\text{m}/\text{cycle}$ probable for short cracks near the inner radius of the discs.

To create instructions of how to avoid the collapse of the brake discs, a number of estimations are necessary. The approximated service life of a truck and the maximum size of an initial defect in the brake discs are already given. This means that the load situation (which gives the growth rate) and the maximum crack length remain.

The truck is supposed to descend the steep slope used in calculations every 200 km, this is reasonable due to the severe load case with the steepness of the slope and big difference in heat input between the outer and inner parts of the disc. Other loads are neglected due to the decrease in crack growth created through overload during the substantial loadings.

Even if the crack growth rate is about constant to start with, at some point the length of the crack will cause an acceleration of the growth rate. To make an estimation of when this

will happen is complicated. As a way to estimate this crack growth rate when the crack has grown for some distance, the results originating from the submodel that replicates the crack used in testing are used. To start with the values supposed to be used during testing can be studied (3, 4 and 5 mm crack length and a straight crack front, see appendix B); here a decrease in growth is shown for longer cracks. Then a submodel of the type used to simulate the test crack, with a 9 mm long crack is made, this has to be taken as a rough estimation because the length of the crack in this case would be long enough to affect the disc globally, and it is hence not suited for submodelling. But the trend is clear even at this length; the stress intensity is decreased. This reasoning leads to the estimation that the crack will grow at a constant rate for at least 10 mm creating a crack length of 13 mm.

Summing up these results gives the service life for the brake disc $5 \cdot 10^5$ km and one replacement of the discs is necessary during the usage of the truck. At more severe usage of the brakes, shorter intervals before replacing the disc are necessary to guarantee that collapse will not occur. Even if only cracks in the surface can be discovered by visual inspection this is recommended every time service is made and it is possible to look at the disc surfaces. To create an increased service life for the discs or to increase the safety, a change in geometry according to the one proposed above or some other way might be the best way. This will probably not make the production of discs more expensive.

The replacement of discs is preferably connected to wear. It is maybe possible to create an instruction connected to the disc thickness when it is time to replace the discs that also considers crack growth. The disc thickness can also have an influence on the crack growth when it is seen that the plastic strain is greater in thinner discs, and that the plastic zone is greater. The influence from the mechanical load is as mentioned earlier the greatest possible source of deviation from the calculated values and this must be considered in further investigations.

7.3 Future Work

Proposals for future work and for the continuation of the work made in this thesis are:

- To get values that better describes the reality concerning the crack growth, a study of what happens after repeated loadings could probably be one of the best ways to refine the model. This is, as mentioned earlier, not possible with the current material model. Another way to get better knowledge about what happens in the discs would be to use the real temperature field applied in small substeps and not ramping the temperature up and down.
- The change in geometry of the spline should preferably be validated by FEM calculations to make sure that it really creates a decrease in plastic strain energy density.

If the change in the affected section is significant, a new submodelling process can be interesting in order to investigate changes in service life prediction.

- One of the most important things in order to continue the work of this thesis is to make real tests on brake discs with defects. A proposed way to do this, combined with calculations on the proposed test model, is described in Appendix B.
- Investigation of how overloading or other post manufacturing methods can be used in order to increase the resistance to crack initiation, and crack growth.
- Further studies of the influence from the simplifications and other sources remarked in the discussion chapter 5.

References

- [1] Ranåker, Måns *Non Linear Material Behaviour of Cast Iron In Disc Brakes -Survey and Calculations*, Divison of Machine Design, Design Sciences, LTH, Lund, 2001.
- [2] ANSYS Homepage <http://www.ansys.com>
www.ansys.com/industry/nonlinear/ANSYS_61_Nonlinear.ppt (2004 09)
- [3] University of Oulu ANSYS 6.1 Manual
<http://www.oulu.fi/atkk/tkpalv/unix/ansys-6.1/content/index.html> (2004 11)
- [4] Anderson, T.L. *Fracture Mechanics Fundamentals and Applications, Second Edition* CRC Press LLC, Florida, 1995.
- [5] Ottosen Saabye, Niels & Ljung, Christer *Strength of Materials and solid Mechanics, AK2*, Division of Solid Mechanics LTH, Lund, 2001.
- [6] Smallman, R.E & Bishop, R.J *Modern Physical Metallurgy & Materials Engineering* Butterworth Heinemann, Oxford, 1999.
- [7] Sundström, Bengt *Handbok och formelsamling i Hållfasthetslära*, Institutionen för hållfasthetslära, KTH, 1998.
- [8] Härkegård, Gunnar *Spricktillväxt under utmattningsbelastning – en översikt, hållfasthetslära* KTH, Stockholm, 1973.
- [9] ANSYS 8.1 Help files
- [10] eFunda, Engineering Fundamentals <http://www.efunda.com/>
http://www.efunda.com/formulae/solid_mechanics/fracture_mechanics/fm_epfm_J.cfm (2004 12)
- [11] Askeland, Donald R *The Science and Engineering of Materials* Stanley Thornes, Cheltenham, 1998.
- [12] Bringas, John E. & Wayman, Michael L. *CASTI Metals Black Book - European Ferrous Data (Fifth Edition) PDF Lite version* CASTI Publishing INC, Edmonton, 2003
<http://www.casti.ca/>
http://www.casti.ca/books_ebooks/lite/BlackBookEuroLite.pdf (2004 11)
- [13] Fa. Fritz Winter GmbH & Co.KG *Erstmusterprüfbericht VDA, Inhaltstoffe von Zukaufteilen (Materialdatenblatt)*, Stadtallendorf, 2003
- [14] Bulloch, J.H. *Near threshold fatigue behaviour of flake graphite cast irons microstructures*, Elsevier, Ireland, 1995

- [15] Department of Mechanical & Industrial Engineering, University of Illinois
<http://www.mie.uiuc.edu/>
<http://www.mie.uiuc.edu/content/files/FCP%202001%20Basic%20Short%20Course/3%20Modeling.pdf> (2004 12)
- [16] Davis, Joseph R. et al *ASM Metals Handbook vol 1*, ASM International, USA, 1995.
- [17] Angus Harold T. *Cast Iron: Physical and Engineering Properties*, Butterworth & Co, London, 1976.
- [18] Ottosen Saabye, Niels & Ristinmaa, Matti *The Mechanics of Constitutive Modelling vol 1*, Division of Solid Mechanics LTH, Lund, 1999.
- [19] Gripemark, Joakim *Non-Linear FE-Analysis of Discs in 19,5" and 21" Fixed Calliper Brakes*, Haldex, Landskrona, 2004.
- [20] Wallin, Mattias *Haldex, Sprickberäkning av bromsskivor*, Altair Engineering, Lund, 2004.
- [21] Mattias Wallin M.Sc., Altair Engineering, Ideon Lund, Telephone +46 46 286 20 56
www.altair.se (2004 10 20, 2005 02 11)
- [22] Jia, X.M. & Dai, F. *Three-Dimensional Static and Dynamic Stress Intensity Factor Computations Using ANSYS*, <http://www.simwe.com/>
<http://www.simwe.com/jour/cae/p001002.pdf> (2004 10)
- [23] Fett, T. *Kink angle in Knoop- and Vickers-damaged glass for spontaneous and subcritical crack growth under mixed mode loading* Institut für Materialforschung II, Karlsruhe, Germany, 2003
- [24] Dahlberg, M *Fatigue crack propagation in nodular graphite cast iron* International Journal of Cast Metal Research, 2004
- [25] Vedmar, Lars *Maskinelement, Transmissioner* Lunds Tekniska Högskola, Lund, 2002
- [26] Fierro, V.E., Sikora, J.A., Aguera, F.R. et al. *Fractomechanical Properties of As-Cast and Austempered SG Cast Iron Between -40 °C and +20 °C*, Materials Research, São Carlos Argentina, 2002
- [27] Thomas J.J, Charkaluk, E. et al *Thermomechanical design in the automotive industry*, Blackwell Publishing, 2004
- [28] Charkaluk, E & Constantinescu, A *An energetic approach in thermomechanical fatigue for silicon molybdenum cast iron*, Materials at High Temperatures, 2000
- [29] S.G.Hong, Samson Yoon, S.B.Lee, *The effect of temperature on low-cycle fatigue behavior of prior cold worked 316L stainless steel* International Journal of Fatigue, 2003

A Material model

The following material model for grey cast iron is written in the form of an ANSYS APDL-file using the ANSYS cast iron model. The stress-strain curves for the three temperatures are shown in figure 24.

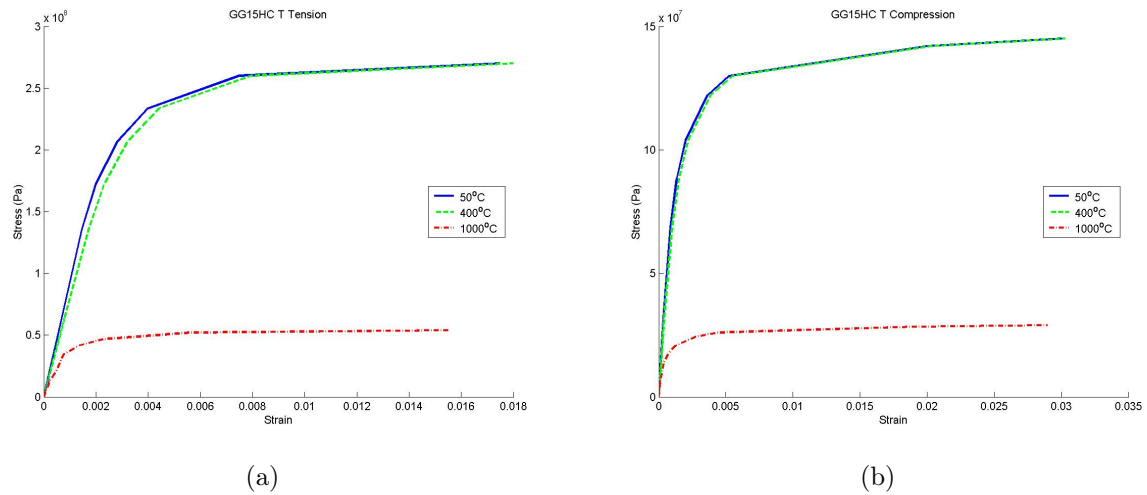


Figure 24: Stress-strain curves in tension and compression for grey cast iron.

```

TOFFST,273                                !Temperatures given in degrees Celsius

MPTEMP,1,20                                !Conductivity (W/(m K))at 20, 700 and 1000 degrees Celsius
MPTEMP,2,700
MPTEMP,3,1000
MPDATA,KXX,1,,53
MPDATA,KXX,1,,48
MPDATA,KXX,1,,45.79

MPTEMP,1,20                                !Specific heat (J/(K Kg)) at 20,700 and 1000 degrees Celsius
MPTEMP,2,700
MPTEMP,3,1000
MPDATA,C,1,,500
MPDATA,C,1,,870
MPDATA,C,1,,1033

MPTEMP,1,20                                !Density at 20 Degrees Celsius (kg/m^3)
MPDATA,DENS,1,,7100

MPTEMP,1,50                                !Elastic values, Young's modulus (Pa) and Poisson's ratio at
MPTEMP,2,400                                !50, 400 and 100 degrees Celsius
MPTEMP,3,1000
MPDATA,EX,1,,9.25e10
MPDATA,EX,1,,7.8868e10
MPDATA,EX,1,,5.55e10
MPDATA,PRXY,1,,0.25
MPDATA,PRXY,1,,0.25
MPDATA,PRXY,1,,0.25

```

```

MPTEMP,1,20                                !Thermal Expansion (1/K) at 20, 700 and 1000 degrees Celsius
MPTEMP,2,700
MPTEMP,3,1000
MPDATA,ALPX,1,,9e-6
MPDATA,ALPX,1,,13.5e-6
MPDATA,ALPX,1,,15.5e-6

TB,CAST,1,3,,ISOTROPIC                    !CAST model, material number 1, 3 temperatures, isotropic input
TBTEMP,20                                  !Plastic Poisson's ratio given at 20 degrees Celsius
TBDATA,1,0.04

TB,UNIAXIAL,1,3,9,TENSION                  !Uniaxial input for material number 1, 3 temperatures, 9 points,
!isotropic input
TBTEMP,50.0                                !Temperature = 50.0 Degrees Celsius
TBPT,,0.000344973,31.91e6                 !Strain = 0.000344973, Stress = 31.91e6 Pa
TBPT,,0.000876865,68.90e6
TBPT,,0.001349595,88.30e6
TBPT,,0.002000162,103.8e6
TBPT,,0.003629919,122e6
TBPT,,0.005260405,130e6
TBPT,,0.020000135,142e6
TBPT,,0.029999568,145e6

TBTEMP,400.0                               !Temperature = 400.0 Degrees Celsius
TBPT,,0.0004046,31.91e6                   !Strain = 0.0004046, Stress = 31.91e6 Pa
TBPT,,0.001005612,68.90e6
TBPT,,0.001514592,88.30e6
TBPT,,0.002194123,103.8e6
TBPT,,0.003857888,122e6
TBPT,,0.005503324,130e6
TBPT,,0.020265477,142e6
TBPT,,0.030270515,145e6

TBTEMP,1000                               !Temperature = 1000 Degrees Celsius
TBPT,,0.000114955,6.38e6                 !Strain = 0.000114955, Stress = 6.38e6 Pa
TBPT,,0.000380288,13.78e6
TBPT,,0.000713198,17.66e6
TBPT,,0.001252054,20.76e6
TBPT,,0.00275064,24.40e6
TBPT,,0.004323468,26.00e6
TBPT,,0.018976712,28.40e6
TBPT,,0.028954523,29.00e6

TB,UNIAXIAL,1,3,8,COMPRESSION              !Temperature = 50.0 Degrees Celsius
TBTEMP,50.0                                !Strain = 0.000689946, Stress = 63.82e6 Pa
TBPT,,0.000689946,63.82e6
TBPT,,0.001469838,135.96e6
TBPT,,0.001999784,172.4e6
TBPT,,0.002829676,206.8e6
TBPT,,0.004000486,233.7e6
TBPT,,0.007489811,260e6
TBPT,,0.017489919,270e6

TBTEMP,400.0                               !Temperature = 400.0 Degrees Celsius
TBPT,,0.0008092,63.82e6                 !Strain = 0.0008092, Stress = 63.82e6 Pa
TBPT,,0.001723893,135.96e6
TBPT,,0.002321931,172.4e6
TBPT,,0.003216103,206.8e6
TBPT,,0.004437179,233.7e6
TBPT,,0.007975648,260e6

```

TBPT,,0.017994442,270e6

TBTEMP,1000.0

!Temperature = 1000.0 Degrees Celsius

TBPT,,0.00022991,12.76e6

!Strain = 0.00022991, Stress = 12.76e6 Pa

TBPT,,0.00048991,21.19e6

TBPT,,0.000757261,34.48e6

TBPT,,0.001339225,41.36e6

TBPT,,0.002316162,46.74e6

TBPT,,0.005615937,52.00e6

TBPT,,0.015543973,54.00e6

B Testing

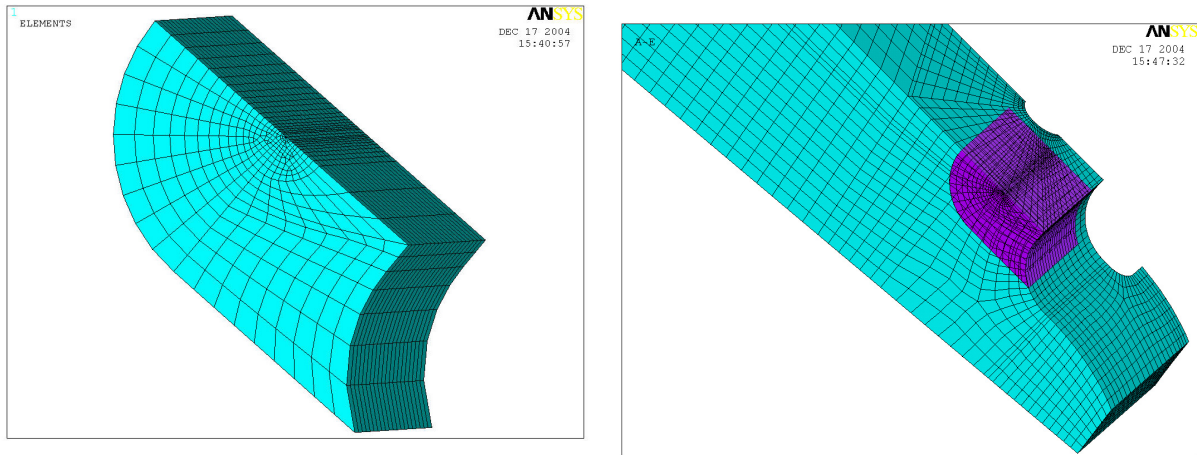
The most important thing to do in subsequent development of the Wave Spline in order to make it fail safe in a fracture mechanical view, is to validate the results from the FEM calculations. A number of simplifications are made through out the calculations and how these influences the results are important to know.

A good way to verify the results from this work would be to let a disc with an in advance created crack go through an accelerated test cycle like the one used as load case earlier. Such test can start with a machined crack, but a crack created by grinding will probably not have a tip that is sharp enough. To make a sharp crack the machined crack has to be loaded a number of cycles, this will make it grow and thereby get a sharp tip. It is important that the loading is made at a level well below the one that will be used later in the testing, to avoid phenomena connected to overloading (see chapter 3.3). When a realistic crack is created this must be measured to know the depth before the real cycling begins.

Measurement of crack length in the spline region can be a delicate task because of the complex geometry. This makes it impossible to measure the crack opening by strain measurement on the body surface. The fixtures necessary when loading the disc probably makes it impossible to measure crack length during growth, and the brake most likely have to be disassembled before measurement. Determination of crack length before start of the test procedure has to be made by some kind of non destructive testing. If the crack has the same length through all the disc thickness it might be possible to measure it by inspection of the length at the disc surfaces. Otherwise some kind of radiography might be necessary.

The problem with measuring crack growth during load makes it necessary to decide an appropriate number of load cycles before the testing starts. After the test cycling both non destructive testing and metallography, or in the case with the constant crack length – inspection can be used in order to find the crack length. Then can the value for the crack growth rate for example be used to adjust parameters, or refine the model in other ways.

To make the prediction, a half submodel is created and placed between two cogs with an equal distance to each cog. The crack is placed in the symmetry plane between the cogs making it possible to create only half the FE-model. The crack length is constant through all of the disc thickness, or at least the part that is covered by the submodel. The submodel does not reach the outer surface of the disc due to the complex geometry here, instead a free surface is modelled a small distance from the real. Doing this is possible due to the submodelling procedure and the fact that the interesting values are found in the middle of the disc, far from the surface. The submodel and the placement of it is shown in figure 25. The calculations follow the methods described in chapter 4.2 and the crack growth rates are calculated as earlier using a linear interpolation between Bulloch's equations (7). The results are shown in table 7.



(a) Submodel

(b) Placement

Figure 25: The submodel and the placement of it in the disc when making the calculations on the test model. The image of the placement is just made to show how the submodel is placed. When making the calculations the submodel is totally free from the full model.

Crack length mm	K_I warm MPa \sqrt{m}	K_I cold MPa \sqrt{m}	ΔK_I MPa \sqrt{m}	R	$\frac{da}{dN}$ μm
3	30.4	10.2	20.2	0.34	33
4	25.3	8.70	16.6	0.34	12
5	22.5	7.07	15.4	0.31	2.5

Table 7: Results from the test geometry calculations.

Results from the calculations show that the growth rate is highly dependent on the crack length; this makes it tempting to define the crack growth rate as a function of the crack length:

$$\frac{da}{dN} = f(a)$$

Doing this makes it possible to find out how many cycles necessary for the crack to grow a certain distance from a_0 to a through derivation:

$$N = \int_{a_0}^a \frac{1}{f(a)} da$$

Taking the function $f(a)$ as two linear fittings between the three points gives two functions describing the number of cycles for different crack lengths:

$$N = \frac{\ln\left(\frac{-0.0208a+95.0}{-0.0208a_0+95.0}\right)}{-0.0208} \quad 3000 \leq [a, a_0] \leq 4000$$

$$N = \frac{\ln\left(\frac{-0.0093a+49.3}{-0.0093a_0+49.3}\right)}{0.0093} \quad 4000 \leq [a, a_0] \leq 5000$$

With the crack lengths given in μm . It shall be pointed out that this creation of a function and the integration of it is just a way to make the values from the calculations useful in tests; it has no theoretical background as such. The choice of a linear fit between the calculated growth rates is just the simplest way to connect the points, and the growth is in reality described by a much more complicated function. To find a function that describes the growth in a more accurate way several more submodels have to be created. The work creating these models will almost certainly not stand in proportion to the gain in accuracy of the resulting values.

In table 7 the values for the stress intensity of the shortest crack are shown. These values are high compared to the ones derived in the tests by Bulloch (see chapter 3.2). This creates some uncertainty of the correctness of the growth rate. The load situation used in calculations is a source of uncertainty when a different loading can create great deviation in growth rate.

C ANSYS APDL files

In the following appendix some of the files used in the ANSYS calculations, concerning the second model, are listed. The files are all written in ANSYS Parametric Design Language (APDL). In table 8 all files used are listed, some of these files are included below:

Files read	Files written
all	
spline_____	
elements_material_lin	spline.rst
wave_390_20_12200_GG15T_struct	spline.db
disp_DiscCooling	
stress_DiscCooling	
submodel_rad_____	
elements_material_lin	submodel_rad.node
	submodel_rad.db
boundary_____	
spline.db	boundary.cbdo
submodel_rad.node	boundary.rst
submodel_rad.db	boundary.db
splineII_____	
elements_material_lin	splineII.rst
wave_390_20_12200_GG15T_struct	splineII.db
temp_BrakesOn2	
splineII.rst	
disp_BrakesOn2	
boundaryII_____	
submodel_rad.db	submodelIII_all.node
boundary.rst	submodelIII_surf.node
outpt_____	submodelIII.db
spline.db	boundaryII.bfin
pathfile.resu	boundaryII.cbdo
splineII.rst	boundaryII.rst
submodelII_all.node	boundaryII.db
submodelIII_surf.node	
boundaryII.cbdo	
boundaryII.bfin	
substres.ist	
post_____	
	postresult.resu

Table 8: The order in which files are used when making the calculations on the second model.

```
!!!!!!!!!!!!!!!!!!!!!!!!!!!!!!!!!!!!!!!!!!!!!!!!!!!!!!!!!!!!!!!!!!!!
!  
! All  
! File used to run through all of the files in the solution  
! schedule.  
!  
!!!!!!!!!!!!!!!!!!!!!!!!!!!!!!!!!!!!!!!!!!!!!!!!!!!!!!!!!!!!!!!!!!!!
```

```
/CWD,'H:\exjobb\spline'  
  
/INPUT,spline,ansys  
/INPUT,submodel,ansys  
/INPUT,boundary,ansys  
/INPUT,splineII,ansys  
/INPUT,boundaryII,ansys  
/INPUT,post,ansys
```

```
!!!!!!!!!!!!!!!!!!!!!!!!!!!!!!!!!!!!!!!!!!!!!!!!!!!!!!!!!!!!!!!!!!!!
!  
! Spline  
! File used to read model and solution for the once loaded  
! disc from text files.  
!  
!!!!!!!!!!!!!!!!!!!!!!!!!!!!!!!!!!!!!!!!!!!!!!!!!!!!!!!!!!!!!!!!!!!!
```

```
!Finish all earlier work and start new project called spline.  
FINISH  
/CLEAR,START  
/CWD,'H:\exjobb\spline'  
/FILENAME,spline,0  
/PREP7
```

```
!Read element type and material model.  
/INPUT,elements_material_lin,ansys
```

```
!Read disc geometry  
/NOPR  
/INPUT,wave_390_20_12200_GG15T_struc_changed,ansys  
/GOPR
```

```
!Scale model to meters  
/PREP7  
ALLSEL  
NSCALE,,ALL,,1/1000,1/1000,1/1000  
FINISH
```

```
!Solve the model to create a result file  
/SOLU  
SOLVE  
FINISH
```

```
!Make changes in the result file using imported solution.  
/POST1  
SET,LAST  
/GRAPHICS,FULL
```

```
/NOPR
/INPUT,disp_DiscCooling,ansys
/INPUT,stress_DiscCooling,ansys
/GOPR
RAPPND
```

```
SAVE
/EOF
```

```
!!!!!!!!!!!!!!!!!!!!!!!!!!!!!!!!!!!!!!!!!!!!!!!!!!!!!!!!!!!!!!
!
! Submodel_rad
! File used to create the geometry and mesh of the submodel.
!
!!!!!!!!!!!!!!!!!!!!!!!!!!!!!!!!!!!!!!!!!!!!!!!!!!!!!!!!!!!!!!
```

```
!Finish all earlier work and start new project called submodel_rad.
```

```
FINISH
/CLEAR,START
/CWD,'H:\exjobb\spline'
/FILNAME,submodel_rad,0
/PREP7
```

```
!Set geometry parameters for the submodel.
crr=3                                !crack radius
crzonew=2.2                          !crack zone width
crzoneh=3                             !crack zone height
!Crack maximum width (crack is given a finite width to simplify the modelling work).
crw=0.001
```

```
!Define material properties and element types.
/INPUT,elements_material_lin,ansys
```

```
!Keypoints used to define local coordinate system with respect to the global used in the full model.
K,1, 120.4716555704,0, 8.571940557153      !crack end at inner surface
K,2, 0,0,0                                !disc centre
K,3, 120.83417368907,0 , 6.3326510151607    !corner between symmetry surfaces
```

```
CSKP,12,1,2,1,3
CLOCAL,11,0,120.7762309429652
```

```
CSYS,11
K,8,0,-1,0
```

```
CSYS,0
!Keypoints used to define a line at the edge of the spline. This line is approximated as a b-spline.
K,10, 120.81690667416,0, 6.6397200416822
K,11, 120.79963964302,0, 6.9467893779677
K,12, 120.78237261187,0, 7.2538587142532
K,13, 120.76237492388,0, 7.4796757896019
K,14, 120.72645721439,0, 7.7036270345929
K,15, 120.62249308499,0, 8.1446384150197
K,16, 120.4716555704,0, 8.571940557153
K,17, 120.2717195436 ,0, 8.9785912859527
```

```
K,18, 120.02544764549,0, 9.3589716595919
K,19, 119.73969616044,0, 9.7106045173713
K,20, 119.41766908954,0, 10.029534978738
K,21, 119.05772959882,0, 10.3049648911
K,22, 118.67035092285,0, 10.539991143381
K,23, 118.25988862798,2.2328313820E-08, 10.731980156071
K,24, 117.82973344894,2.2296069030E-08, 10.874478408676
```

```
CSYS,11
K,16,0,-crw,0
```

```
!Changed to create the width of the crack.
```

```
!First edge part
FLST,3,8,3
FITEM,3,3
FITEM,3,10
FITEM,3,11
FITEM,3,12
FITEM,3,13
FITEM,3,14
FITEM,3,15
FITEM,3,1
BSPLIN, ,P51X
```

```
!Second edge part
FLST,3,9,3
FITEM,3,16
FITEM,3,17
FITEM,3,18
FITEM,3,19
FITEM,3,20
FITEM,3,21
FITEM,3,22
FITEM,3,23
FITEM,3,24
BSPLIN, ,P51X
```

```
!Plane used to define crack mesh in symmetry plane of disc.
WPCSYS,,11 !Defines the working plane location based on CSYS.
!Create the area in the middle symmetry plane of the disc.
BLC4,crr,0,crr,crzonew
BLC4,crr,0,crr,-crzonew
BLC4,crr/4,0,3*crr/4,crzonew
BLC4,crr/8,-crw,crr/8,-crzonew+crw
BLC4,crr/8,0,crr/8,crzonew
AGLUE,ALL
```

```
L,4,34
L,9,33
L,32,24
L,16,35
L,1,36
L,3,39
```

```
AL,8,9,16,23
AL,2,10,11,18
AL,1,12,13,22
```

```
K,100,crr/8,0,crr/8
K,101,crr/8,-1,crr/8
K,102,crr,0,crr/8
```

```
!Circle (and straight line) used as drag path using the VDRAG command symbolising crack front.
```

```

CIRCLE,100,7*crr/8,101,102,90
L,4,26
NUMMRG,ALL

!Mesh areas with MESH200 elements in the symmetry plane
TYPE,2
ESIZE,0.8
KSCON,4,0.1,1

AMESH,1
AMESH,6

ESIZE,0.2
AMESH,7
AMESH,2

LESIZE,20,,2

!Create volumes from meshed areas.
TYPE,3
VDRAG,1,2,6,7,,20
VDRAG,13,18,21,25,,19

!Change the element type from MESH200 to SOLID95
ESEL,S,TYPE,,3
TYPE,4
EMODIF,ALL
ALLSEL

!Create volumes at the inner radius
CSYS,11
VEXT,3,,,,crr/4
VEXT,5,,,,crr/4
VDRAG,43,,,,59
KMODIF,66,crr/8,-crzonew,crr

NUMMRG,KP
VDRAG,48,,,,69
NUMMRG,KP
VDRAG,61,,,,56
NUMMRG,KP
VDRAG,57,,,,51

!Create areas and volumes to fill up the rest of the model.
AL,17,37,60,81
AL,27,47,70,88
AL,80,15,39,62
AL,72,49,28,89
NUMMRG,KP
VA,46,4,32,15,70,72
VA,41,24,51,71,8,73
NUMMRG,KP

!Free mesh created volumes.
ESIZE,0.5
MSHKEY,0
MSHAPE,1,3D
TYPE,4
VMESH,9,16

!Write nodes and elements to text files, detaching them from areas and rebuild the model.
ALLSEL
CSYS,0

```

```
NWRITE
EWRITE
VCLEAR,ALL
ACLEAR,ALL
VDELE,ALL,,1
NREAD
ERead
```

```
!Delete all area elements.
ESEL,S,TYPE,,2
EDELE,ALL
ALLSEL
NUMCMP,ALL
```

```
!Scale the model to meters
ALLSEL
CSYS,0
NSCALE,,ALL,,1/1000,1/1000,1/1000
```

```
!Write the nodes to text file
NWRITE
```

```
!Save the database
SAVE
/EOF
```

```
!!!!!!!!!!!!!!!!!!!!!!!!!!!!!!!!!!!!!!!!!!!!!!!!!!!!!!!!!!!!!!!!!!!!
!
! Boundary
! File used to create a deformed submodel symbolising the
! volume around the crack in the once heated disc.
!
!!!!!!!!!!!!!!!!!!!!!!!!!!!!!!!!!!!!!!!!!!!!!!!!!!!!!!!!!!!!!!!!!!!!
```

```
!Finish all earlier work and start new project called boundary.
FINISH
/CLEAR,START
/CWD,'H:\Exjobb\spline'
/FILNAME,boundary,0
```

```
!Read the full model with modified results
RESUME,spline,db
/POST1
FILE,spline,rst
SET,,,,,2
```

```
!Write interpolated deformation to file 'boundary.cbdo' for all nodes in the submodel
CBDOF,submodel_rad,node
```

```
!Read the submodel geometry and mesh
FINISH
/CLEAR,START
RESUME,submodel_rad,db
/CWD,'H:\Exjobb\spline'
/FILNAME,boundary,0
```

```

FINISH

/SOLU
CSYS,0
ANTYPE,STATIC
TREF,50

!Write deformations to all submodel nodes
/NOPR
/INPUT,boundary,cbdo
/GOPR

!Set geometric boundary conditions at the middle symmetry surface
CS,11,0,43835,43845,43843
NSEL,S,LOC,Z,-0.01/1000,0.01/1000
NSEL,R,EXT
DSYM,SYMM,Z,11,

!Solve model to get a resultfile with the plastic deformations in the submodel
ALLSEL
SOLVE

SAVE
/EOF

```

```

!!!!!!!!!!!!!!!!!!!!!!!!!!!!!!!!!!!!!!!!!!!!!!!!!!!!!!!!!!!!!!!!!!!!!!
!
! SplineII
! File used to read model and solution for the disc in the
! end of the second loading from text files.
!
!!!!!!!!!!!!!!!!!!!!!!!!!!!!!!!!!!!!!!!!!!!!!!!!!!!!!!!!!!!!!!!!!!!!!!

```

This file is essentially the same as spline, and hence not included. The only difference between the two files is that another solution is used. The temperatures in the disc are imported instead of the stresses.

```

!!!!!!!!!!!!!!!!!!!!!!!!!!!!!!!!!!!!!!!!!!!!!!!!!!!!!!!!!!!!!!!!!!!!!!
!
! BoundaryII
! File used to make the crack calculations on the submodel.
!
!!!!!!!!!!!!!!!!!!!!!!!!!!!!!!!!!!!!!!!!!!!!!!!!!!!!!!!!!!!!!!!!!!!!!!

```

```

!Finish all earlier work and start new project called boundaryII.

FINISH

```

```

/CLEAR,START
/CWD,'H:\exjobb\spline'
/FILNAME,boundaryII,0

!Read the solved submodel and reset it in the deformed condition making the plastic deformations permanent.
RESUME,submodel_rad,db
/PREP7

UPGEOM,1,LAST,LAST,boundary,rst

!Write all nodes in the deformed submodel to a file
ALLSEL
NWRITE,submodelIII_all,node

!Write the surface nodes in the deformed submodel to a file
CS,11,0,43835,43845,43843

NSEL,S,LOC,Y,crzone*0.98/1000,crzone*2/1000
NSEL,A,LOC,Y,-crzone*0.98/1000,-crzone*2/1000
NSEL,A,LOC,X,1.98*crr/1000
CLOCAL,12,1,,,,,90
NSEL,A,LOC,X,1.98*crr/1000,3*crr/1000
NSEL,R,EXT

CSYS,0
NWRITE,submodelIII_surf,node

!Save the deformed submodel database
SAVE,submodelIII,db

!Read the file created for the transfer of residual stresses to the submodel.
/INPUT,outpt,ansys

!Clear the model and reload splineII with solution to the database.
FINISH
/CLEAR,START
/CWD,'H:\exjobb\spline'
/FILNAME,boundaryII,0

RESUME,'splineII','db'

/POST1
FILE,splineII,rst

!Write interpolated temperatures and displacements for the submodel node coordinates to a text file.
BFINT,submodelIII_all,node
SET,,,,,2
CBDOF,submodelIII_surf,node

!Clear the model and reload submodelIII to the database.
FINISH
/CLEAR,START
/CWD,'H:\exjobb\spline'
/FILNAME,boundaryII,0
RESUME,'submodelIII','db'

/SOLU
ALLSEL
!Apply the displacements at the surface nodes of the submodel, and the temperature field on all nodes.
/NOPR
/INPUT,boundaryII,cbdo

!Set geometric boundary conditions at the middle symmetry surface

```

```
CS,11,0,43835,43845,43843
NSEL,S,LOC,Z,-0.01/1000,0.01/1000
NSEL,R,EXT
DSYM,SYMM,Z,11,
```

```
ALLSEL
```

```
/INPUT,boundaryII,bfin
!Read residual stresses in the submodel from file created by outpt.
ISFILE,READ,substres,ist
/GOPR
```

```
SOLVE
SAVE
/EOF
```

```
!!!!!!!!!!!!!!!!!!!!!!!!!!!!!!!!!!!!!!!!!!!!!!!!!!!!!!!!!!!!!!!!!!!!
!
! Outpt
! File used to read residual stresses from the full model
! and write them to an ISTRESS file.
!
! The submodel database is supposed to loaded before start
! reading this file.
!
!!!!!!!!!!!!!!!!!!!!!!!!!!!!!!!!!!!!!!!!!!!!!!!!!!!!!!!!!!!!!!!!!!!!
!Open/create the file 'pathfile.resu' for writing
*CFOPEN,pathfile,resu
CSYS,0

!Get the maximum element number for element type 5 (minimum element number 1 required)
*GET,nelm,ELEM,, NUM,MAX,

pathpt=1001
turn=1
!Looping over all elements
*DO,i,1,nelm

!!Maximum number of points in a path is 1000 and looping is necessary!!!!!!!!!!!!!!!!!!!!!!!!!!!!!!!!!!!!
*IF,pathpt,EQ,1001,THEN
pathpt=1

*IF,nelm-turn*1000,GE,0,THEN
*VWRITE,turn,1000
PATH, centerpts%i, %I, 10, 0
*ELSE
pts=nelm-(turn-1)*1000
*VWRITE,turn,pts
PATH, centerpts%i, %I, 10, 0
*ENDIF

turn=turn+1
*ENDIF
```

```

!!!!!!!!!!!!!!!!!!!!!!!!!!!!!!!!!!!!!!!!!!!!!!!!!!!!!!!!!!!!!!!!!!!!!!!!!!!!!!!!!!!!!!!!!!!!!!!!!!!!!!!!!!!!!!!!!!!!!!!!
!Get the coordinates for the element centroid
*GET,center_x,ELEM,i,CENT,X
*GET,center_y,ELEM,i,CENT,Y
*GET,center_z,ELEM,i,CENT,Z

!Write the element centroids to the file, 'pathfile.resu', like path point creating command
*VWRITE,pathpt, center_x, center_y, center_z
PPATH, %I, , %G, %G, %G
pathpt=pathpt+1

!When 1000 points are created in the path commands to map stresses are added to the file, 'pathfile.resu'.
*IF,pathpt,EQ,1001,OR,i,EQ,nelm,THEN
*VWRITE
PDEF, ,S,X,AVG
*VWRITE
PDEF, ,S,Y,AVG
*VWRITE
PDEF, ,S,Z,AVG
*VWRITE
PDEF, ,S,XY,AVG
*VWRITE
PDEF, ,S,YZ,AVG
*VWRITE
PDEF, ,S,XZ,AVG

!/EOF does not break, it is just written to the file, 'pathfile.resu'.
*VWRITE
/EOF
*ENDIF
*ENDDO

!Stop writing to the file 'pathfile.resu'.
*CFCLOSE

!Write parameters to a file to preserve 'nelm'
PARSAV,SCALAR
RESUME,spline,db
PARRES
/POST1
FILE,spline,rst
SET,,,,,2

!Open/create the file 'substress.ist' for writing.
*CFOPEN,substres,ist

linnr=1
count=1
!Loop due to the limitation of points in a path.
*DO,j,1,nelm/1000+1

!Read a path from 'pathfile.resu', stresses get mapped to the path due to the commands in the file read.
/INPUT,pathfile,resu,,linnr

!Get the number of points in the path read.
*GET, numpts, PATH, 0, NODE

!Loop over the points in the path reading the stresses mapped to it.
*DO,i,1,numpts

*GET, str_x, PATH, 0, ITEM, SX,PATHPT,i
*GET, str_y, PATH, 0, ITEM, SY,PATHPT,i

```

```

*GET, str_z, PATH, 0, ITEM, SZ,PATHPT,i

*GET, str_xy, PATH, 0, ITEM, SXY,PATHPT,i
*GET, str_yz, PATH, 0, ITEM, SYZ,PATHPT,i
*GET, str_xz, PATH, 0, ITEM, SXZ,PATHPT,i

!Write stresses in the form required for the command ISTRESS to the file 'substress.ist'.
*VWRITE,count
eis, %I, 0
*VWRITE,str_x,str_y,str_z,str_xy,str_yz,str_xz
%G, %G, %G, %G, %G, %G
count=count+1
*ENDDO

linnr=linnr+1008

*ENDDO

!Stop writing to the file 'substress.ist'.
*CFCLOSE

/EOF

!!!!!!!!!!!!!!!!!!!!!!!!!!!!!!!!!!!!!!!!!!!!!!!!!!!!!!!!!!!!!!!!!!!!!!
!
! Post
! File used to post process solution writing crack intensity
! values to a text file.
!
!!!!!!!!!!!!!!!!!!!!!!!!!!!!!!!!!!!!!!!!!!!!!!!!!!!!!!!!!!!!!!!!!!!!!!
FINISH
/POST1

!Open/create the file 'postresult.resu' for writing,
!writing is done after the last line created in the file.
*CFOPEN,postresult,resu,,APPEND

!Create a local coordinate system in the crack tip and changing the result coordinate system.
CS,17,0,1,4,51
RSYS,17

!Create a path with the points nearest to the crack tip
PATH,symmetri,5,30,20
PPATH,1.,1
PPATH,2,280
PPATH,3,281
PPATH,4,863
PPATH,5,864

!Calculate the stress intensity parameters
KCALC,0,1,3,1           !plane strain, material number 1,full crack model,print CTOD

!Print output to file 'postresult.resu'!!!!!!!!!!!!!!!!!!!!!!!!!!!!!!
*GET,KI,KCALC,0,K,1
*GET,KII,KCALC,0,K,2

```

```

*GET,KIII,KCALC,0,K,3

*VWRITE
Symmetry surface

*VWRITE,KI
Stress intensity value KI %E
*VWRITE,KII
Stress intensity value KII %E
*VWRITE,KIII
Stress intensity value KIII %E %/
!!!!!!!!!!!!!!!!!!!!!!!!!!!!!!!!!!!!!!!!!!!!!!!!!!!!!!!!!!!!!!!!!!!!

!The same thing is done in the middle of the modelled crack front below.
CS,18,0,5176,5360,6640
RSYS,18

PATH,middle,5,30,20

PPATH,1,5176
PPATH,2,9901
PPATH,3,9930
PPATH,4,28806
PPATH,5,28774

KCALC,0,1,3,1           !plane strain, material number 1,full crack model,print CTOD

!Print output to file 'postresult.resu'!!!!!!!!!!!!!!!!!!!!!!!!!!!!
*GET,KI,KCALC,0,K,1
*GET,KII,KCALC,0,K,2
*GET,KIII,KCALC,0,K,3

*VWRITE
Middle of crack

*VWRITE,KI
Stress intensity value KI %E
*VWRITE,KII
Stress intensity value KII %E
*VWRITE,KIII
Stress intensity value KIII %E %/
!!!!!!!!!!!!!!!!!!!!!!!!!!!!!!!!!!!!!!!!!!!!!!!!!!!!!!!!!!!!!!!!!!!!

CSYS,0
RSYS,0
!Stop writing to the file 'postresult.resu'.
*CFCLOSE
/EOF

```